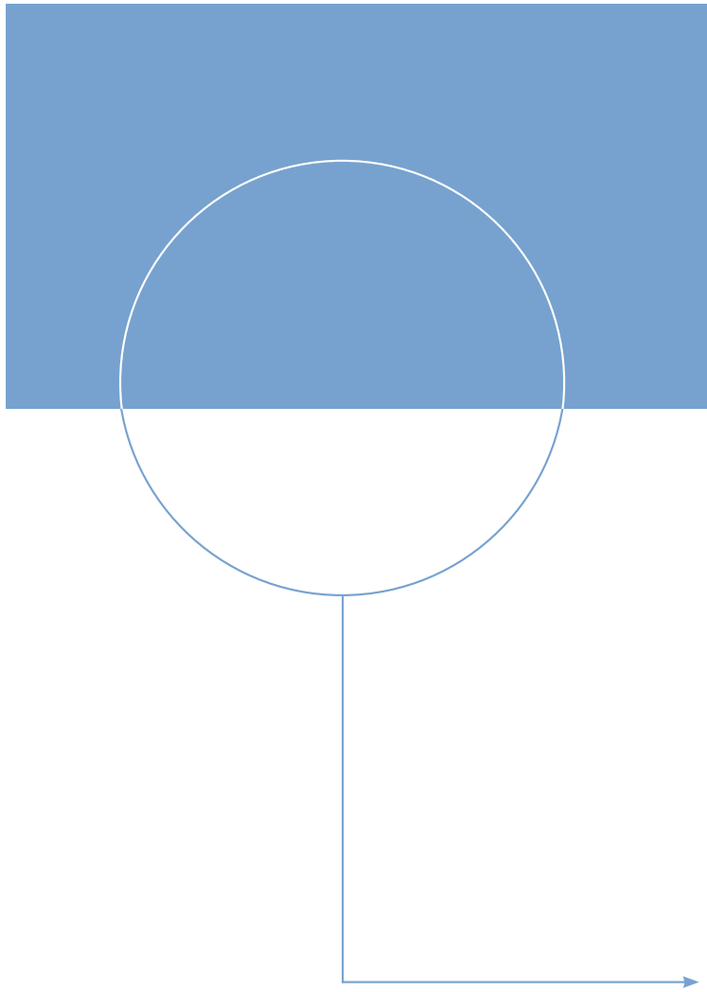

Master's thesis

2019

Erlend Kjøraas

NTNU
Norwegian University of
Science and Technology
Faculty of Engineering
Department of Mechanical and Industrial Engineering

Erlend Kjøraas

The Protection Mechanism of Lead Based Paint

June 2019

NTNU
Norwegian University of
Science and Technology

NTNU
Norwegian University of
Science and Technology

NTNU
Norwegian University of
Science and Technology

The Protection Mechanism of Lead Based Paint

Erlend Kjøraas

Mechanical and Industrial Engineering
Submission date: June 2019
Supervisor: Ole Øystein Knudsen

Norwegian University of Science and Technology
Department of Mechanical and Industrial Engineering

Preface

This master thesis is conducted at the Department of Mechanical and Industrial Engineering at Norwegian University of Science and Technology (NTNU). The thesis is a part of the course TMM4960, and was conducted during the spring 2019. The thesis is a part of a joint project between NTNU, SINTEF and industry partners.

Most importantly I wish to thank my supervisor, Ole Øystein Knudsen. Further I wish to thank Amin Hossein Zavieh, Catalina H. Musinoi Hagen, Silje Marie Dale and Sigurd Wenner, for help performing tests and as helpful discussion partners. I want to express my gratitude to Ann-Karin Kvernbråten and Nils-Inge Johan Nilsen at SINTEFs corrosion for advice given for sample preparations.

Trondheim, 11 June 2019

Erlend Kjøraas

Abstract

This master thesis aims to reveal the corrosion protective mechanism of lead-based paint (LBP). Previous research indicates that the protective mechanism could be due to presence of lead species on the surface of the steel. Which kind of lead components and in what quantities they exist could be important to describe the true protection mechanism.

Four different instruments has been used for investigation of the surface oxide under the LBP; X-ray photoelectron spectrometry (XPS), scanning kelvin probe (SKP), transmission electron microscope (TEM) and X-ray diffraction (XRD).

Lead is found in all of the characterisation tests (XPS, TEM and XRD). From XPS and SKP, following conclusion can be made:

- Inhibition of corrosion can be associated with a more noble corrosion potential, from the theoretical equilibrium potential of steel at -0.44V vs. SHE to the observed corrosion potential at -0.25V vs. SHE in SKP.
- This potential corresponds to the reduction reaction of lead, at a concentration of approximately 10^{-4}M. Cathodic deposition seems like a possible deposition method of lead. An alternative deposition method could be precipitation deposition of lead monoxide/hydroxide.
- Cathodic deposition will lead to a depolarisation of the reduction reaction, and the steel will be protected due to anodic protection.
- Other mechanism such as a high resistance surface oxide due to the presence of lead oxide or a barrier of metallic lead on the electrodes could be an explanation for the protection. A combination of all three presented protection mechanisms could be a possibility.

Sammendrag

Denne masteroppgaven har til hensikt å belyse blymønjes beskyttende mekanisme mot korrosjon. Det har tidligere vært antatt at tilstedeværelsen av bly på ståloverflaten gir korrosjonsbeskyttelse. Hvilke blykomponenter og mengden vil være viktig for å beskrive de beskyttende egenskapene til jernoksidet.

Fire instrumenter har blitt brukt for å belyse jernoksidets natur. XPS (røntgen fotoelektronspektroskopi), SKP (skanning kelvin probe), TEM (transmisjons elektron mikroskopi) og XRD (røntgen diffraksjon).

Alle karakteriseringsmetodene (XPS, TEM og XRD) viser at bly er til stede. Videre kan følgende konklusjoner dras fra SKP og XPS undersøkelser:

- Inhibisjon av korrosjon kan assosieres med et økt korrosjonspotensial til stål fra -0,44V mot SHE til -0,25V mot SHE.
- Ved dette potensialet vil metallisk bly utfelles på ståloverflaten ved reduksjon av blyioner, ved en antatt konsentrasjon på ca. 10^{-4}M. En alternativ utfellingsmekanisme er konsentrasjonsutfelling av blymonoksid/hydroksid, men mindre sannsynlig.
- Katodisk utfelling av metallisk bly vil føre til at depolarisering av reduksjonsreaksjonen og dermed vil stålet bli anodisk beskyttet.
- Andre mekanismer som en barriere av metallisk bly som hindrer reaksjonene på elektrodene til korrosjonscellen eller en oksid film med høyere motstand mot korrosjon pga. tilstedeværelsen av blyoksider i overflateoksidet. En kombinasjon av alle nevnte mekanismer er tenkelig.

Content

Abbreviation

Ac	Acetate
AES	Auger Electron Spectroscopy
CD	Cathodic Disbonding
EDS	Energy-Dispersive X-ray Spectroscopy
ELLD	Electron-Energy Loss Spectroscopy
LBP	Lead-Based Paint
NTNU	Norwegian University of Science and Technology
PDF	Power Diffraction File
SCE	Saturated Calomel Electrode
SHE	Standard Hydrogen Electrode
SKP	Scanning Kelvin Probe
TEM	Transmission Electron Microscopy
XPS	X-Ray Photoelectron spectroscopy
XRD	X-Ray Diffrection

1. Introduction

1.1 Background and Motivation

Lead based paint (LBP) is a simple and economical paint, which has good anti corrosive properties. However, lead is toxic, and LBP has not been used in Norway since the mid 70s. LBP is often used with a simple one-component binder like linseed oil or alkyd and is therefore an easy paint to work with. Figure 1.1 shows Golden Gate Bridge, which until 1965 was painted with red lead in a linseed oil carrier [1]. Figure 1.2 shows Bakke Bru in Trondheim, built in 1929, also originally painted with LBP. Both bridges have the characteristic red/orange colour.

Figure 1.1: Golden Gate Bridge[2].

Figure 1.2: Bakke Bru in Trondheim from 1929 [3].

Research on the protection mechanism of LBP are from early 90s, and older. However, the mechanism of inhibition is still of scientific interest. A better comprehension of the protection mechanism of LBP, could be useful for development of new "green" organic coatings.

Previous research finds the most likely mechanism [4] to involve deposition of lead species, which bring about passivation of the steel surface underneath the paint film. However, few articles confirm that lead is present on the steel surface. Instrumentation for characterisation has developed considerably in the last 25-30 years. Therefore, modern instruments offer a greater sensitivity and will give a better representation of the true nature of the steel surface.

The preliminary work [5] during this project found that lead species are present in the surface oxide under LBP. Figure 1.3 shows the Pb 4f peak for the XPS scan. The peak is found at 138.8 eV, both before sputtering and after different sputtering times. It was identified as lead oxide, without any further information about the oxidation state of the lead. No difference with respect to the iron oxide composition was observed between painted samples and un-painted samples. However, the method for removal of paint from the steel surface prior to XPS investigation was found to be questionable. It was concluded that other methods should be tried, e.g. mechanical removal.

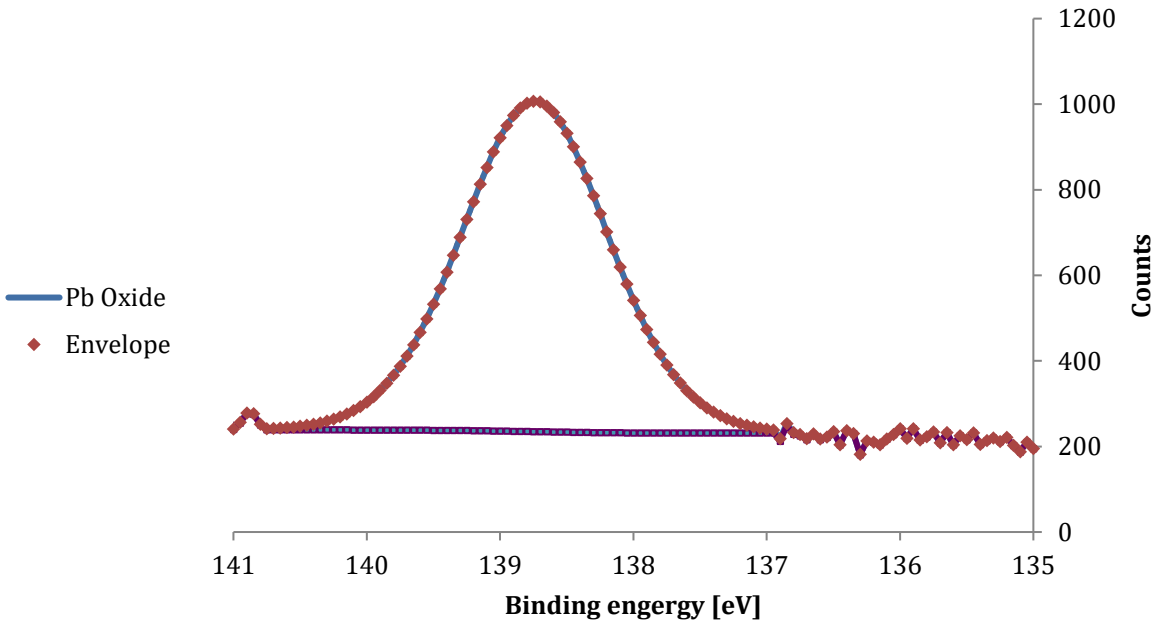

Figure 1.3: Pb 4f peak before sputtering [5].

1.2 Problem Description and Objective

As mentioned in section 1.1, characterisation of the protected steel surface is of interest. Metals resistance against corrosion is often associated with the native oxide of metals. Properties that can describe the nature of the protective oxide underneath the LBP are therefore important. Such properties are:

- Thickness of the protective oxide
- Porosity of the protective oxide
- Oxidation state of the elements in the oxide, both for lead and iron
- Semi-conductive properties of the film
- Incorporation of lead species in the protective oxide

The objective of this thesis is to examine the protective oxide on the steel surface, with the goal of revealing information of the listed properties. Different characterisation methods will be used for this purpose.

1.3 Limitations

Inhibition of corrosion on steel by pigments in paint can occur due to two main mechanisms; due to formation of protective oxide film or due to a change of the environment at the paint-steel interface [6]. Previous research in mind, the objective of this thesis only considers the first mentioned form of inhibition. Protection due to change in environment (pH) will not be considered. Some theories for the protection mechanism of LBP are based on the formation of unsolvable components with aggressive ions, such as chloride and sulphur, which will not attack the steel surface [6]. This theory will not be considered during this thesis.

1.4 Contributions

Several persons perform the practical work presented in this report. The author performed the sample preparation for XPS, XRD and SKP examination. Sr. Eng. Amin Hossein Zavieh at NTNU performed examination in XPS, while department Eng. Silje Marie Dale at NTNU performed the XRD examination. PhD candidate Catalina H. Musinoi Hagen (NTNU) performed the SKP examination. Results from XPS, XRD and SKP was analysed by the author. Researcher Sigurd Wenner at SINTEF performed sample preparation, examination and analysis in TEM.

2. Theory

2.1 Passivation of Metals

Historically there has been presented two theories for passivation of metals. The first one states that a passive film is formed from reaction products, such as oxides, and provides a diffusion barrier [7]. An argument in favour of this theory is the correlation between a typical thickness of 30Å and passivation. The correlation between measured polarisation curves and theoretical thermodynamically stabile oxides is also put forward as argument for this theory [8].

The second theory is a process where absorbed species (e.g. oxygen) forms a film on the metal surface, which depress absorption of water molecules on the metallic surface. Since the water phase is displaced from the metallic surface, anodic dissolution is inhibited. These films are noticeable thinner than films associated as barrier films, and an absorbed monolayer is observed to have a passivating effect [7]. However, Bardal [8] emphasises that these layers over time will grow and form a thicker oxide layer, and therefore the difference between the two theories is not necessarily large.

A protective oxide can be divided in three different types. The first one will depress both anodic and cathodic reactions, since transportation of ions and electrons are hindered. Aluminium oxide will typically behave like this. The second one will hinder transport of ions trough the oxide, but not electrons due to the semiconducting nature of these oxides. Examples are oxides formed at Cr, Ni and Fe. This group of oxides are often thinner, which allows them to lead electrons trough the film. However, both oxides will prevent corrosion, since both electrodes is needed to form a corrosion cell. The third type of layer will partially inhibit both anodic and cathodic reactions. This layer is formed by precipitation from the electrolyte, and they are typically more porous than the two other oxides. A classical example is rust [8].

The key factors of the protective quality of an oxide are often determined by the ability for transportation of ions and the solubility of the oxide. Ion conductivity is strongly related to the porosity of the oxide [8]. Iron oxides tend to be more porous compared to

aluminium oxides, and therefore aluminium will resist corrosion better than carbon steel in most environments. The mechanical strength and the adhesion to the metallic surface are also important for a well functioning oxide film [8].

Destruction of the passive film can occur by different mechanisms. Mechanical wear will break down the passive film, and the metals ability to re-passivate under a given condition will determine if corrosion will occur. Chemical breakdown is due to a change in pH, temperature or concentration of aggressive ions in the electrolyte. Electrochemical breakdown is due to a change in potential, where the material is moved from a passive or immune state to active state as given in a Pourbaix-diagram [8].

2.2 Organic Coatings

Organic coatings or paint is normally considered to consist of five different groups of components: Pigments, binder, fillers, additives and solvent. The two most important are the binder and the pigments. They determine the protective properties, considering corrosion. The *binder* is in most cases an organic polymer. The purpose is, as the name indicates, to form a film and that adhers to the surface that shall be protected. Acrylics, alkyds, epoxies, polyesters, polysiloxanes and polyurethanes are examples of binders. These different binders will give the coating film different protective properties, such as for example mechanical strength, adhesion to surface and ability to transport ions [6].

Pigments are the other main component determining the protective properties against corrosion for a coating. The purpose of adding pigments is to hinder corrosion and/or to give the coating colour. Pigments protect the metallic surface against corrosion in three ways; as a barrier, trough cathodic polarisation or as an inhibitive pigment. [6]

To see the coating as a physical barrier between the corrosive water phase and the metallic surface is a common explanation for corrosion protection. However, all paint will to some extend allow migration of water and oxygen ion trough the film. A more accurate explanation of the true protection mechanism is to look at it as a *stabilisation of the metallic oxide* under the paint. Paint will strongly limit the permeability of ions

trough the film, which prevents dissolution of the protective oxide. Prevention of a stabile water phase present on the metallic surface will also prevents corrosion. A pigment may act as a barrier by increasing the diffusion path length for ions through the paint film. Since the purpose of a barrier pigment is to make the diffusion path longer, the pigment should have a flake shape. Aluminium flakes are a typical barrier pigment[6].

The next type of pigments is sacrificial pigments. This kind of pigment protects by acting as an anode in a galvanic cell with the metallic surface, similar to cathodic protection with anodes on steel structures. In contrast to the barrier pigments, the sacrificial pigment has to be in sufficient electrical contact with the metallic surface [6]. Experience has shown that it needs at least 80wt% zinc in the film in order to achieve this property[9].

Inhibitive pigment protects against corrosion by:

- Changing the environment, by modification of pH
- Stimulate the growth/formation of a protective surface

Inhibitive or passivating pigment act as reservoir in the coating. Like for the sacrificial pigments, inhibitive pigments need to be in contact (or close to) with the metallic surface. This is important because these active pigments only work in contact with the surface or electrolyte, and the paint is therefore functioning as a reservoir of inhibiting pigments [6].

2.3 Lead Based Paint

LBP is a paint where lead oxides are used as a protective pigment. The most used pigment historically is red lead, Pb_3O_4. According to information given to Statens vegvesen by Jotun, LBP contained about 1.2 kg red lead per litre wet paint [10]. The vehicle used together with red lead was first linseed oil, and later alkyd. Various lead salts and white lead oxide was also used as colour pigments, but then in much smaller concentrations. The use of lead based colour pigments lasted longer than the use of red lead protective pigment due to the lower concentration. However, lead is found to be highly toxic and is for that reason not used anymore.

2.3.1 Alkyd

Alkyd is a one-component resin, which cure in air. The resin is therefore easy to work with, and it is relatively cost effective. On the negative side, the alkyd paints are not suitable for use on alkaline surfaces. An alkaline environment will lead to saponification, hence acid and alcohol is formed during degradation of the binder. However, alkaline pigment, such as red lead, can react with acids in the resin and thereby strengthen the protective paint film [6]. Another issue with the use of an alkyd is that they contain alcohol, which is water soluble, and therefore the alkyd paints tend to absorb water and swell. Hence, alkyd paints may lose adhesion to the surface if they are submersed[6].

2.3.2 Red lead

The protective pigment for LBP is red lead, Pb_3O_4. The structure of red lead is Pb_2PbO_4 or $2PbO \bullet PbO_2$ as shown in Figure 2.1. Red lead is a mixture of Pb(II) and Pb(IV) and has a characteristic orange/red colour. The pigment can contain up to 15% free lead monoxide, and it is “observed” increased corrosion resistance with increased content of free PbO in the red lead LBP [11].

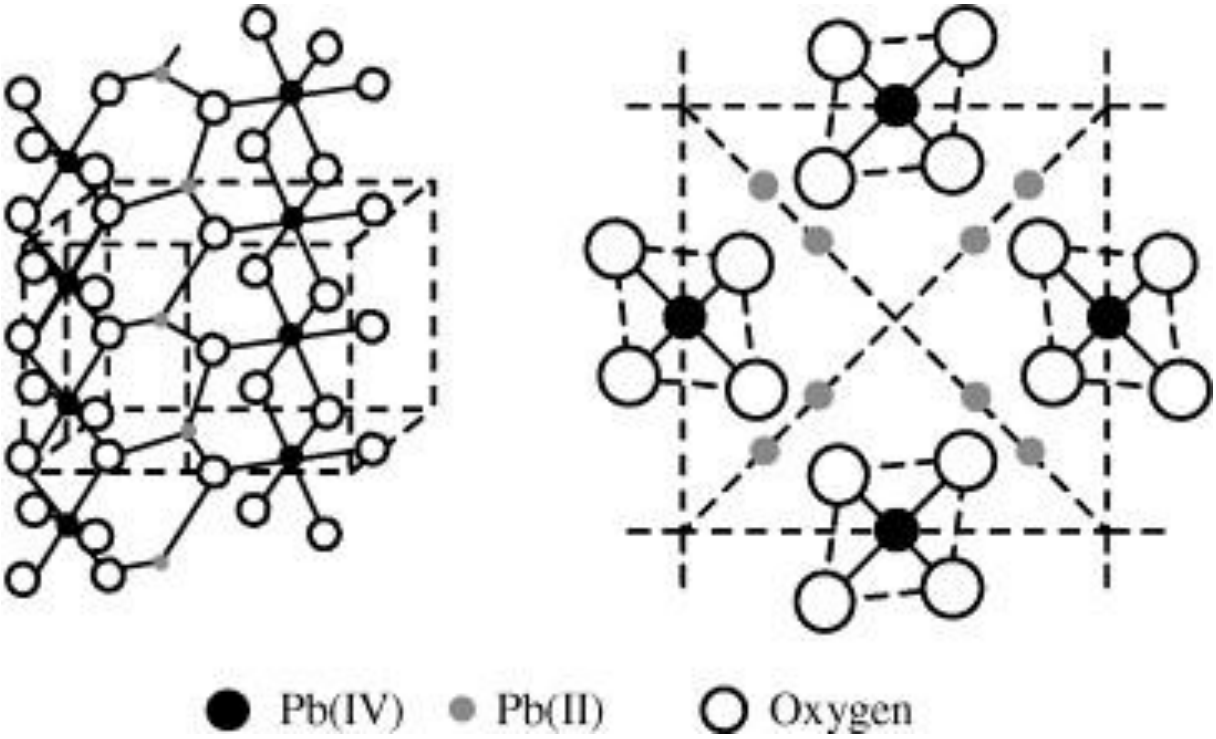

Figure 2.1: Chemical structure of red lead [12].

Red lead and PbO_2 is considered as insoluble in water, while PbO has a solubility of 20mg/L [13]. However, Brokbartold et al. [14] has reported that the solubility of red lead in ultra pure water is 68.5 mg/L. The solubility of LBP was examined in the same paper. LBP was cured on glass panels before the film was scratched of and ball-milled into a powder. This powder showed a solubility of 18.3mg/L and 6mg/L at pH equal to 3 and 5 after 70 days in the test solution [14]. Figure 2.2 shows the Pourbaix diagram for lead in water at 25^0C. The area for lead hydroxide is found in the same area as lead monoxide and is for the sake of simplicity just noted as PbO [15]. Figure 2.3 shows the close relation between the solubility of PbO and $Pb(OH)_2$.

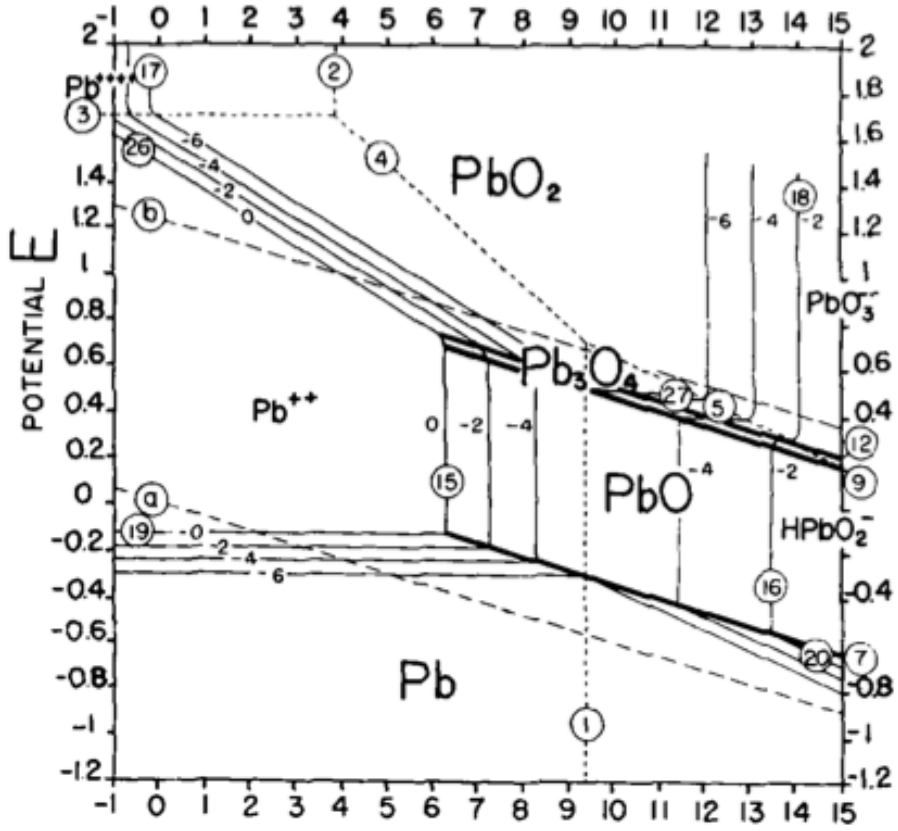

Figure 2.2: Pourbaix diagram of lead in water at 25^{0}C [15].

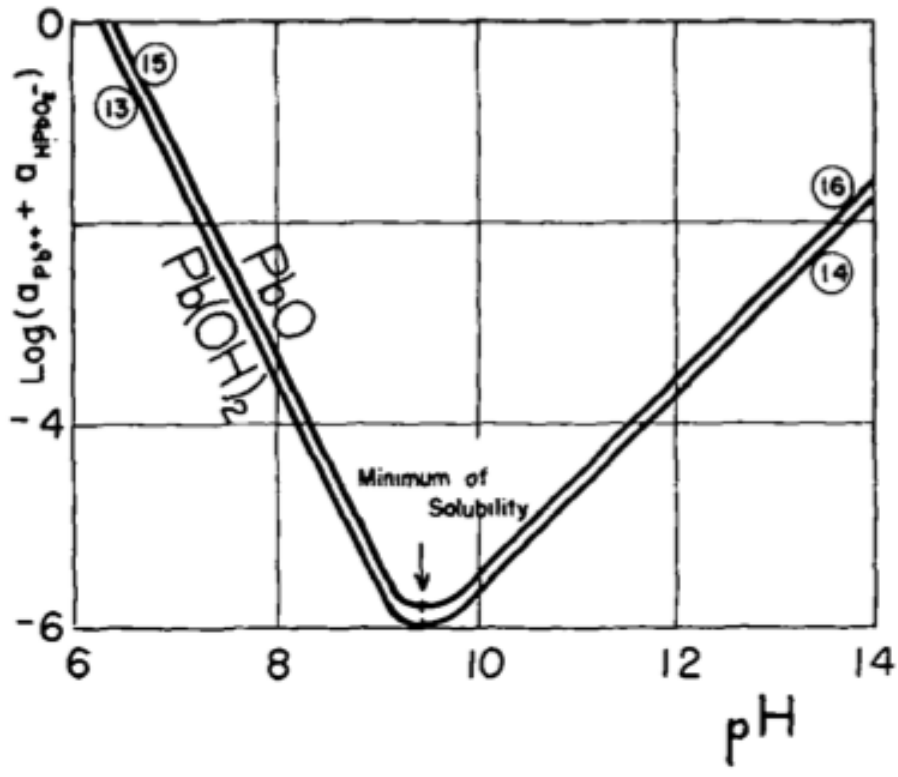

Figure 2.3: Solubility of PbO and $Pb(OH)_2$ vs. pH [15].

Some of the lines in the Pourbaix-digram (Figure 2.2) can be described as following [15]:

(19): $Pb^{2+} + 2e^- \Leftrightarrow Pb_{(s)}$, $E_0 = -0.126 + 0.0295 \log (a_{Pb^{2+}})$ (Eq. 1)

(7): $PbO + 2H^+ + 2e^- \Leftrightarrow Pb_{(s)} + H_2O$ $E_0 = 0.248 - 0.0591\ pH$ (Eq. 2)

(15): $PbO + 2H^+ \Leftrightarrow Pb^{2+} + H_2O$ $log\ (a_{Pb^{2+}}) = 12.67 - 2.0\ pH$ (Eq. 3)

In addition, Alwards and Findlay´s SI Chemical Data give [13]:

$PbO + 2H_2O + 2e^- \Leftrightarrow Pb_{(s)} + 2OH^-$ $E_0^0 = -0.58V$ (Eq. 4)

E_0^0 is the standard electrode potential, E_0 is the equilibrium potential and $a_{Pb^{2+}}$ is the activity of lead ions.

2.3.3 Protection Mechanisms

Several possible protection mechanisms have been proposed. Mickalonis and Leidheiser [16] and Lindqvist [17] have listed some:

- Chemical reaction between lead oxide and the steel substrate, which lead to passivation [17].
- Improved mechanical properties of the paint film due to formation of lead soaps [16, 17].
- The pigment forms an alkaline environment under the paint [16, 17].
- Redox properties of absorbed lead species inhibit the anodic dissolution of iron [16, 17].
- Under the corrosion process of iron, the red lead forms a precipitated layer on both anodic and cathodic sites. This layer act as a diffusion barrier [17].
- Red lead pigmented film act as a barrier to acidic gasses [16, 17].
- Reduced ion permeability trough the coating, hence protection is due to barrier properties [16].
- Deposited metallic lead will maintain the growth of ferric oxide film, followed by re-oxidation of lead. The deposited lead act in a catalytic manner [16].
- Degradation products of lead soaps inhibit corrosion, by depolarisation of the oxygen reduction. The protective ferric oxide is stabilised and thickened [16, 17].
- Lead reaction with sulphur, to form insoluble components [16].

Mickalonis and Leidheiser [16] found the last three as the most likely mechanisms. Thomas [18] did not found any correlation between the sulphate in rusted steel and lead, and therefore concluded that the protection mechanism is not formation of insoluble components of aggressive anions. Later Thomas [19] found that the transportation of water through the coating is sufficiently high for corrosion to occur. Hence, LBP do not resist corrosion through great barrier properties.

The soap theory has gained a lot of support through the years and is mainly based on work done by Mayne and co-workers [4, 20, 21]. Mayne [22] showed that lead soaps formed by reaction between lead oxide and linseed oil can prevent corrosion of steel in water. Later Mayne and Rooyen [23] found that lead, calcium and sodium salts extracted from azelates, a degradation product of the lead soaps, was inhibiting at a pH of 4.6-5, but at lower azelate concentration in the case of lead salts. Salts formed by suberic acid and peloargonic acid were also found inhibitive.

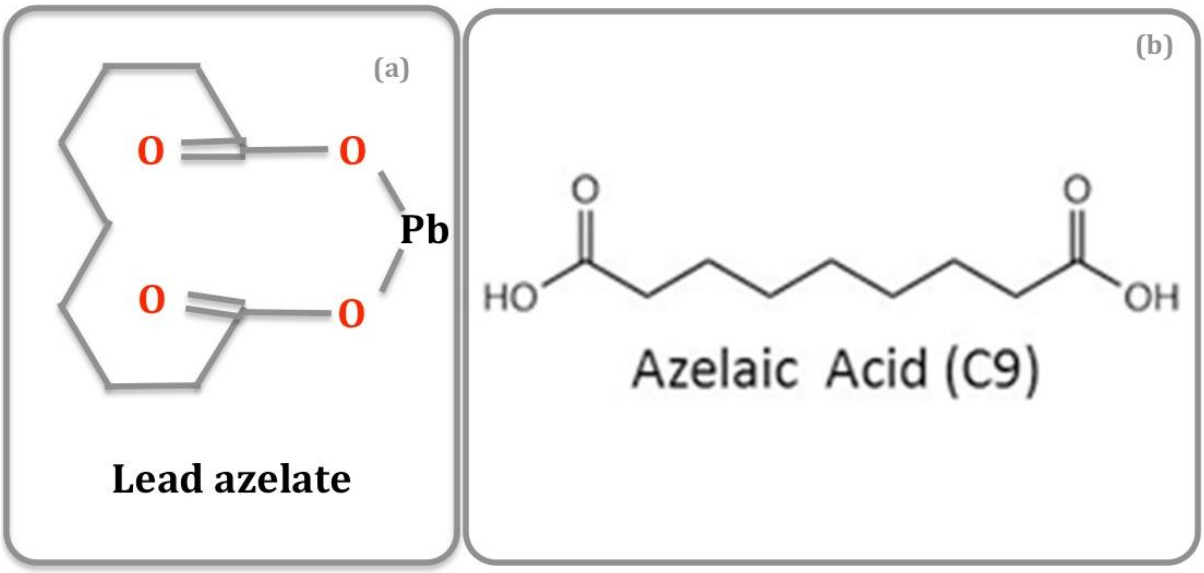

Figure 2.4: The structure of lead azelate (a) [24] and azelaic acid (b) [25].

Linseed oils consist mainly of a mixture of long chained fatty acids [26]. Mayne and Ramshaw [26] have showed that lead salt of these acids was found to be inhibitive, and a chain length of 8-9 carbon atoms seems to be ideal for inhibition. Lead azelate, as shown in Figure 2.4, is the major extract of the lead soaps and the protective properties are largely determined by its presence.

According to Appleby and Mayne [4] 5-20ppm lead azelate is sufficient to make water inhibitive. They argued that the inhibition is due to the growth of the iron oxide, since a 7.2-16.9% thicker oxide where calculated from observed potential measurements. The growth was assumed to be due to lead species, as the same growth was not observed for sodium and calcium azelate[4].

A hypothesis presented by Appleby and Mayne [4] is that ionic lead is reduced to metallic lead on cathodic sites on the surface, by being an alternative cathodic reaction

instead of oxygen reduction. Metallic lead will depolarise the oxygen reaction and provide a sufficient current density for ferric oxide growth. This thickening will take place until the film is adequately thick for prevention of anodic dissolution[4].

Later Appleby and Mayne [21] looked at the protection efficiency of different binders. Four different binders (linseed oil, alkyd, oiticica and tung oil) with red lead were tested. Inhibition was achieved when the lead content was equal to 25ppm for linseed oil, 37ppm for oiticica and 62ppm for alkyd. Tung oil did not bring about inhibition of corrosion. The authors stress the relation between the vehicles ability to form azelaic acid, where linseed oil will produce the greatest amount of azelaic acid, then oiticica, alkyd and tung oil accordingly[21].

Mayne [22] has shown that litharge (PbO), red lead and lead powder is inhibitive in distilled water, where litharge is found to be the best followed by red lead and then lead powder. Lead dioxide did not give any inhibition. These observations have later been confirmed by Pryor [27]. Through polarisation measurements,
Lindqvist and Vannerberg [17] found that steel is passivated in a slurry mix of pigmented red lead and a 0.1M $NaClO_4$ solution. Both the anodic and cathodic reactions where inhibited. No inhibition was observed during submersion in 0.1M NaCl. From SEM analysis and X-ray diffraction (Guinier method), metallic lead where found. In an alkaline solution, metallic lead was rapidly covered by a layer of oxides, hydroxides and carbonates. Ionic lead is reduced to metallic lead on the surface, and this thin layer will hinder the oxygen reduction reaction, according to Lindqvist and Vannerberg [17].

Later Lindqvist [28] tested a galvanic cell between lead and iron, with that purpose of finding the initial behaviour of the cell. Again, he used 0.1M sodium chloride and 0.1M sodium perchlorate as electrolyte. Interestingly, at pH larger than five, he found that lead acted as an anode for some hours, before a change in potential occurred. For pH lower than 4 iron immediately acted as anode, which he related to the formation of hydrogen at the cathode. The potential of corroding iron allows ionic lead in the electrolyte to be reduced on the surface to metallic lead. Initially, during the deposition, a repair of the iron oxide and probably oxidation from ferrous to ferric oxide will occur due to the depolarisation. Subsequently a potential change will oxidise the metallic lead,

while iron is cathode. If this theory is true, metallic lead has a catalytic effect. It is also not expected that metallic lead will be accumulated on/in the iron oxide[28].

Lindquist [28] also measured the dissolution rate of lead from four different vehicles: linseed oil, alkyd (54% linseed oil), chlorinated rubber and epoxy. The measurements took place during a period of 100 days. The dissolution rate was showed to be highest for linseed oil and then alkyd, chlorinated rubber and epoxy in that given order. The binders with dicarboxylic acids, alkyd and linseed oil, showed a dissolution rate 100 times higher compared to binders of epoxy and chlorinated rubber [28].

Mickalonis and Leidheiser [16] examined the inhibitive mechanism of LBP under three different simulated model environments. The first model environment had a relatively large distance between anode and cathode, the second with a small distance and lastly a model without oxygen. The polarisation tests consisted of a galvanic cell of two steel plates submerged in an electrolyte of mix of sodium acetate and ionic lead [16].

The reasoning for the first model was to simulate a difference in pH between anodic and cathodic sites, which is thought to occur if the distance between them is large enough. A steel (anode, pH=4.5)/steel (cathode, pH=10) cell was created. A reduction in cathodic current was observed. This was attributed to inhibition of the oxygen reduction due to lead deposits. Trough XPS and Auger Electron Spectroscopy (AES) metallic and oxidised lead was observed on the cathodic plate. The deposition of these lead species was thought to be due to under-potential deposition (UPD). As explained by Mickalonis and Leidheiser[16]:

> *"The subsequent oxidation of the lead species is related to the thinness of a layer deposited by UPD and the negative free energy associated with the oxidation process. The formation of these deposits by participation appears unlikely since the deposits were not visually observed and the inhibition was potential dependent."*
>
> *(Mickalonis and Leidheiser, p. 35-36[16])*

The second model simulated a small distance between the anodic and cathodic sites, hence pH will approach a neutral value on both anodic and cathodic sites due to a buffering effect. Metallic lead was visually observed on the cathode. At anodic sites

metallic lead and/or lead oxide was observed by XPS and AES. Metallic lead deposits on cathodic sites, increases the current density and leads to increased anodic current. The potential is moved into the passive region where growth of iron oxide will occur. This is observed by a drop in the overpotential for passivation of steel from 690 mV vs. SCE without ionic lead present in the electrolyte to 500 mV vs. SCE with ionic lead present. Figure 2.5 shows the polarisation curve with different concentrations of lead acetate (Ac) [16].

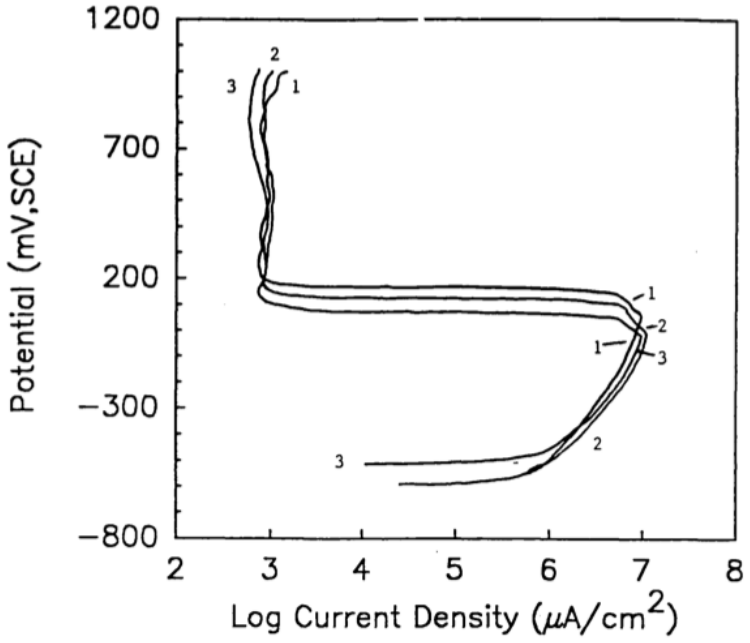

Figure 2.5: Anodic polarisation curve of steel in 0.1M NaAc at pH =4.5, and PbAc concentration of 0M (1), 2×10^{-6}M (2) and 10^{-3}M (3) [16].

The last environment is without oxygen. Under such condition, hydrogen evolution is the driving cathodic reaction for corrosion. Observation of lead on corroding steel surface was observed under deaerated condition. The hydrogen evolution was inhibited, which lowered the corrosion rate [16].

Juttner have attributed inhibition of lead in acidic environment to UPD of metallic lead on the surface. Metallic lead occurs on the steel surface, and low binding energy between lead and hydrogen leads to a lowering in absorption of hydrogen on cathodic sites, which hinder the cathodic reaction. Strong Pb-Pb and Pb-bulk material bindings will also

hinder transfer of ionic iron into the solution, and therefore supress the anodic dissolution [29].

Mickalonis and Leidheiser [16] stresses that the LBP has multiple protection mechanisms. Together with the mechanisms mentioned above, LBP offer a reservoir of lead salt. Lead components such as oxides, hydroxyl, carbonates, sulphates and chlorides have different solubility at different pH, which allow lead cations to be present over a wide pH range. Wetting/drying cycles will lead to an accumulation of these lead components and a reservoir of lead components will exist under the paint [16].

Mayne et al. [20] looked at steel specimens after immersion in lead and calium azelate (10^{-4}M) for 24h, before examination with the use of Auger spectra. They observed a peak identified as some kind of lead species.

The authors discuss three different possible deposition mechanisms. The first one is precipitation of lead cations in the electrolyte. The precipitated ion is most likely $Pb(OH)_2$, since hydroxyl is produced at cathodic sites. The authors find this unlikely because a local pH of 9 or higher is required for precipitation of Pb cations, which is considerable higher than the bulk. The second explanation could be that anionic lead species is deposited, e.g. plumbate. These species are thought to form a ferric salt. But also this seems unlikely, as equilibrium of plumbate in the Pb^{+} containing solution is reached at 10^{-47}M. This quantity of plumbate is not sufficient to inhibit corrosion. The last discussed theory is cathodic deposition of metallic lead. This theory requires a potential of -224mV vs. SHE, before a stabile iron oxide is formed [20]. The metallic lead will cause inhibition as explained earlier of Appleby and Mayne [4].

Even if Mayne et al. believes that the second explanation is not realistic, Revie and Uhling supports this theory.

> *"The inhibiting ion in the case of red lead is probably PbO_4^{4-}, which is released in just sufficient amount to passivate steel, protecting it against rusting by water reaching the metal surface. It is likely that lead oxides and hydroxides of other compositions also have inhibiting properties in this regard, but red lead appears to be the best of the lead compounds."*
>
> *(Revie and Uhling 4ed. Page 291. [7])*

One, of several, theories for inhibition by chromates is based on the present of CrO_4^{2-}. The protection mechanism is due to formation of the complex structure $FeCr_2O_{14-n}(OH^-)_n$. This structure is thought to catalyse a strengthening of the atomic bonding between iron and oxygen and therefore a better protective film is achieved [6].

Similar, Vetere and Romagnoli [30] attribute the main protection mechanisms of LBP to formation of a plumboferrite ($PbFe_4O_7$ or $PbO{\cdot}2Fe_2O_3$) film. They observed plumboferrite by using X-ray diffraction on steel plates submerged in a water solution containing different lead oxides (red lead and lead monoxide). A powder mix of red lead, lead monoxide and iron were used as a reference.

Polarisation of an iron plate was tested in 0.5M sodium perchlorate solutions containing lead monoxide, lead dioxide or red lead. Passivation was achieved in the presence of lead monoxide and red lead, but not for lead dioxide [30].

They also measured the corrosion rate of painted panels, with different binders and pigmented with red lead or red iron oxide (Fe_2O_3). The first binder is oleoresinous and it is saponifiable, while the other one is vinyl and will not lead to saponification. The coating with red lead and the oleoresinous binder gave the best corrosion protection, but red lead in the vinylic coating performed better than the paint pigmented with Fe_2O_3. The electrolyte was 0,5M sodium perchlorate [30].

An Iron panel are passivated when open circuit potential is less negative than -370mV vs. SCE. They conclude that an alkaline medium contributes to the passivation, but formation of plumboferrite is the most important reason[30].

Summarised, it appears that the protection mechanism against corrosion of LBP is the presence of elemental lead on the steel surface. Extracts of linseed oil containing paints (especially lead azelate) is found to be inhibitive on steel when submerged in water[22, 23, 26]. However, lead monoxide and red lead is also found inhibitive in different water solutions [17, 22, 27]. Lead dioxide is not found inhibitive [22, 27, 30].

Several researchers are of the opinion that metallic lead is deposited at the surface and thereby encourage the growth of iron oxide due to depolarisation of the oxygen reaction[4, 16, 28]. Lindqvist [28] have presented a possible explanation for why metallic lead will not be found on the steel surface. Vetere and Romagnoli [30] are of that belief that the protection mechanism of LBP is due to formation of plumboferrite in the iron oxide.

The deposition of lead species is a debated topic. In the paper of Mayne, Turgoose and Wilson [20] three possible mechanisms were discussed: Catodic deposition, precipitation and deposition of anions. Mayne and co-workers [4, 20] is in favour of cathodic deposited of metallic lead on the surface. Several other authors have also attributed the mechanism of deposition to cathodic deposition [16]. A deposition of plumbite or plumbate is also suggested, which is supported by Revie and Uhlig [7] without any detailed explanation of the subsequent inhibition. Lastly deposition due to precipitation is discussed as an option. The most likely precipitants are lead hydroxide. However, Mayne et al. saw this theory as doubtful [20].

3. Method

3.1 Steel Preparation

The steel used was a cold rolled carbon-manganese steel (DC01). The XPS and XRD samples are cut into roughly 10x10mm samples from the initial plate, which has a thickness of 2mm. The samples for SKP are cut into 20x40mm from the same plate.

All samples are first grinded stepwise with paper size 200, 360, 500 and 1200grit. The samples are washed with ethanol between each step. Subsequent polishing of the samples is performed with 3µm SiC particles, before polishing with 1µm particles. Five minutes ultrasonic ethanol bath was performed before, in between and after the two polishing steps.

3.2 X-ray Photoelectron Spectrometry

The characterisation by XPS examination is performed with a Kratos Ultra Axis^{DLD}. A schematic overview of the samples is given in Table 3.1. Sample 1 to 4 is tested at the same time.

3.2.1 Sample preparation

LBP (*MINIO DI PIOMBO RED LEAD PRIMER*®) or Epoxy (JOTAMASTIC 87 ®) is applied to the Sample 2, 3 and 4 with a brush. The samples are left to dry for two days before they are baked (furnace: Fermaks) at 40˚C for three days. Sample 2 to 4 is exposed in a moisture chamber (Vötsch VC 0057) at 40°C and 82% relative humidity for 8 days. The thickness of the two samples was measured to 198µm +/- 14 and 171 +/- 31. Sample 1 is not painted and therefore not exposed to a corrosive environment.

The paint on Sample 3 and parts of Sample 4 was not removed before the examination. Sample 4 has one area with mechanically removed paint. The mechanical removal where performed by applying the paint on two steel specimens which are placed next to each other. After the paint has cured, the cured paint film will hold these two specimens together. After exposure as previous described, one of the specimens where placed in a vise, while the other specimen where broken off. Figure 3.1 shows an illustration of this idea of mechanical removal.

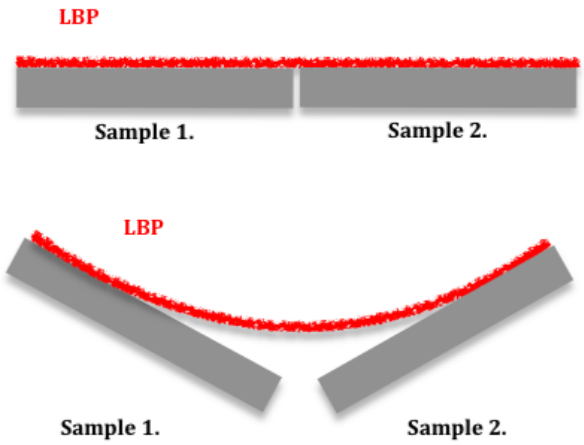

Figure 3.1: Method for mechanical paint removal.

The paint on Sample 2 was removed by a thinner (*Jotun Thinner NO. 17*®). The samples are put in the thinner for one and a half hours. The wet/soft paint is dragged off with a scalpel and then gently wiped with a cotton stick, with the effort to not touch the steel surface.

Table 3.1: Schematic overview of XPS samples.

Sample	Examined in:	Paint	Environmental Exposure	Removal of paint
1	XPS XRD	None	None	-
2	XPS XRD	LBP	82RH, 40°C, for 8 days	By thinner
3	XPS	LBP	82RH, 40°C, for 8 days	None
4	XPS	Epoxy	82RH, 40°C, for 8 days	- By breaking - None

3.2.2 Scanning and Analysis

The samples were loaded into the chamber before the pressure is lowered to 10^{-9} Torr. An Al Kα monochromatic source is used with an emission current of 10mA and anode HT of 10kV. Pass energy of 160eV is used for survey scans, while a pass energy of 20eV is used for regional scans of Pb, Fe, O, and C. Step size is 0.1eV. For sputtering, argon is used at a chamber pressure of $3.1 \bullet 10^{-6}$ Torr whit energy of 3keV. Electrostatic lenses are used.

CasaXPS is used for analyses of the scans. A Shirley background is used. All peaks are corrected according to C 1s (C-C, C-H) located at 285,0 eV.

3.3 Transmission Electron Microscopy

A sample was taken from the old Hell Railway Bridge in Stjørdal, Norway. The bridge was installed in 1902 and was located at the estuary of Stjørdalselva. The bridge was replaced with a new bridge in 2016.

The sample is coated with a 10nm gold layer before it is prepared by FIB (focus ion beam). The sample is mounted to a Cu-grid, and a cross-section of the paint/metal interference is cut out. The sample is then thinned down to approximately 100nm. Picture of the sample was taken, together with EDS (Energy-Dispersive X-ray Spectroscopy) and ELLD (Electron-Energy Loss Spectroscopy).

3.4 Scanning Kelvin Probe

The steel is prepared as described in 3.1. Tape is applied to each side of the polished surface of the samples, letting a stripe of the bare steel surface in the middle. LBP (*MINIO DI PIOMBO RED LEAD PRIMER*®) is applied to the polished bare steel by dripping paint on the area before dragging a flat wooden stick over the whole sample. The samples are cured for one day, before baking at 40^0C for one day. The tape is then removed, and bare steel is exposed on the sides. The finished samples can be seen in the test chamber in Figure 3.2 (with reservoirs, as described in 3.4.2). The SKP test is performed at two different occasions; the first one is tested immediately after baking of the samples (7. February) and the second test performed 11 weeks after baking (25. April). A schematic overview of the samples is given in Table 3.2.

The height regulating SKP are delivered from Wicinski-Wicinsk. Point measurements are performed with a NiCr needle probe. Measured potential is calibrated against a know $Cu/CuSO_4$ electrode (E = 0.320V vs. SHE).

Table 3.2: Schematic overview of SKP samples.

Sample	Paint	Thickness	Environmental Exposure of the Whole Sample	
			Test Round 1	Test Round 2
11	LBP	132µm +/- 60	95RH for 116 hours, RT.	95RH for 166 hours, RT.
12	LBP	120µm +/- 38	95RH for 116 hours, RT.	-
13	LBP	62µm +/- 8	-	95RH for 166 hours, RT.

a: The thickness is measured at different locations on the coated samples and not only at the place where the actual measurements has been conducted. The thickness varies over the whole coated sample.

3.4.1 Point Measurement Test

It was measured 11 potentials at four different locations. The interval between each measurement is 105 minutes. The first measurement is done after 105 minutes after the insertion of the samples into the chamber. At Sample 11, one measurement was performed on the coating and one on the bare steel. The same applies for Sample 12.

The condition under the test is 95 % relative humidity at room temperature. Figure 3.2 shows the two samples in the test chamber.

3.4.2 Cathodic Disbonding Test

The cathodic disbonding (CD) test is performed when a reservoir of 3.5wt% NaCl is introduced as showed in Figure 3.2. The reservoir drop is held in place next to the damage in the coating by three walls (*X60*® two-component glue) as shown in Figure 3.2. The surrounding conditions are as in section 3.4.1, 95%RH at RT. CD measurements is performed by letting the probe pass over the coating in a straight line from the end of the reservoir towards the center of the LBP stripe. A pre-scan of the samples is performed before the CD test, which indicates the potential over the coating at different distances from the reservoir in a protected state. The potential over the reservoir was measured, but only during the first test.

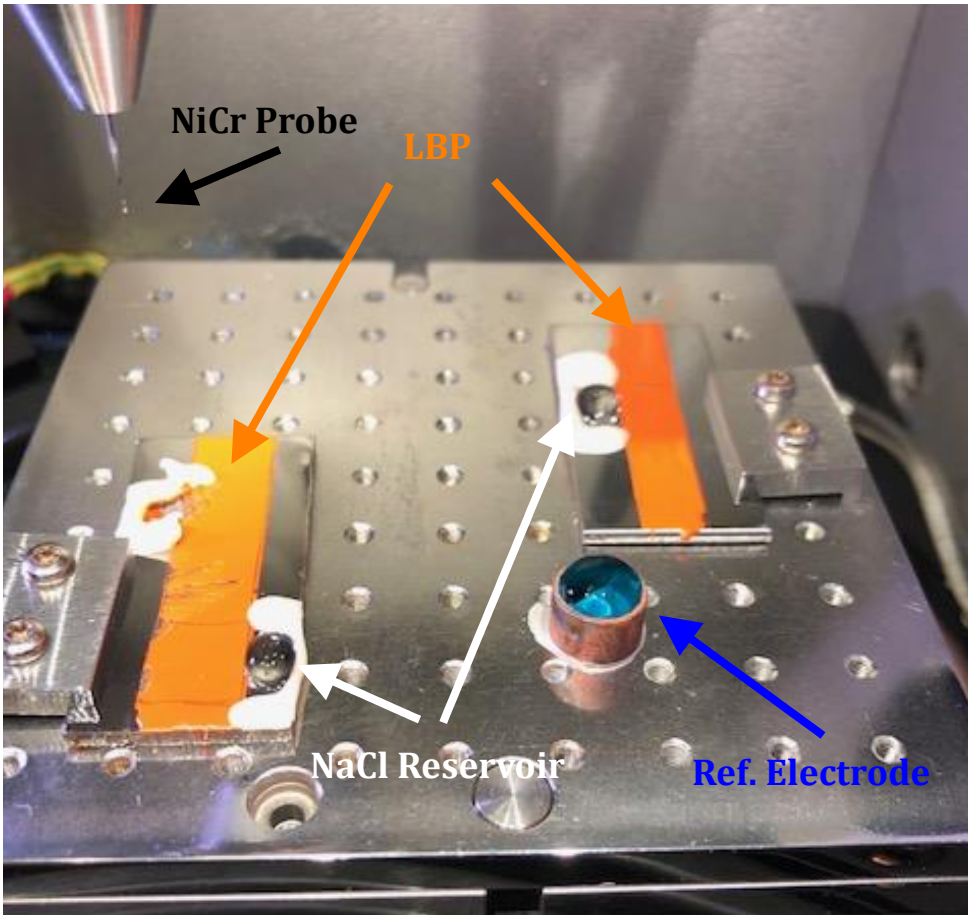

Figure 3.2: Picture of Sample 11 (left) and Sample 13 (right) in the chamber. The reference electrode, NaCl reservoirs, the LBP stripes and the NiCr probe is marked in the picture.

3.5 X-ray Diffraction

Two samples were tested with XRD. The samples used are Sample 1 and 2 as given in Table 3.1. The samples were mounted to the sample holder using modelling clay. Grazing Incidence XRD (D8 A25 Advance DaVinci) is used for the scan. The incident angle is set to 4° and a step size of 0.020°. The scan time is 5 hours and 30 minutes.

4. Results

4.1 X-ray Photoelectron Spectroscopy

Figure 4.1, 4.2 and 4.3 shows the results from the XPS scan of the Pb 4f region of the LBP coating (Sample 3) at 0, 5 and 15 seconds of sputtering time respectively. As it is seen from Figure 4.1, only one peak is found at 138.9eV in the top surface of the paint layer. When moving further down in the paint (Figure 4.2 and 4.3), two peaks are seen. The first peak is located at 137.1eV while the other one is located at 138.6eV. The relation between the areas for the peaks represents the relative amount of the different lead species present in the material. The peak located at 138.6eV makes up approximately two-thirds (5s: 64.6% and 15s: 66.82%) of the lead species, while the peak at 137.1 makes up approximately one-third. As described in subsection 2.3.2 the relation between Pb(II) and Pb(IV) is 2:1, and it is therefore strong indications that Pb(II) is located at 138.6eV and Pb(IV) is located at 137.1eV. The same argumentation has previously been used by Kim et al[31].

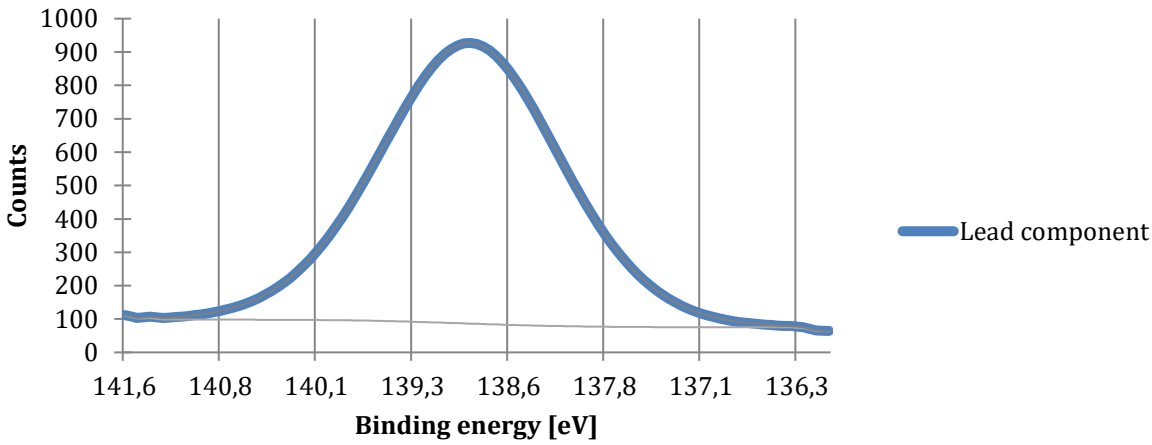

Figure 4.1: Pb 4f region scan of the LBP coating after 0s sputtering. Sample 3.

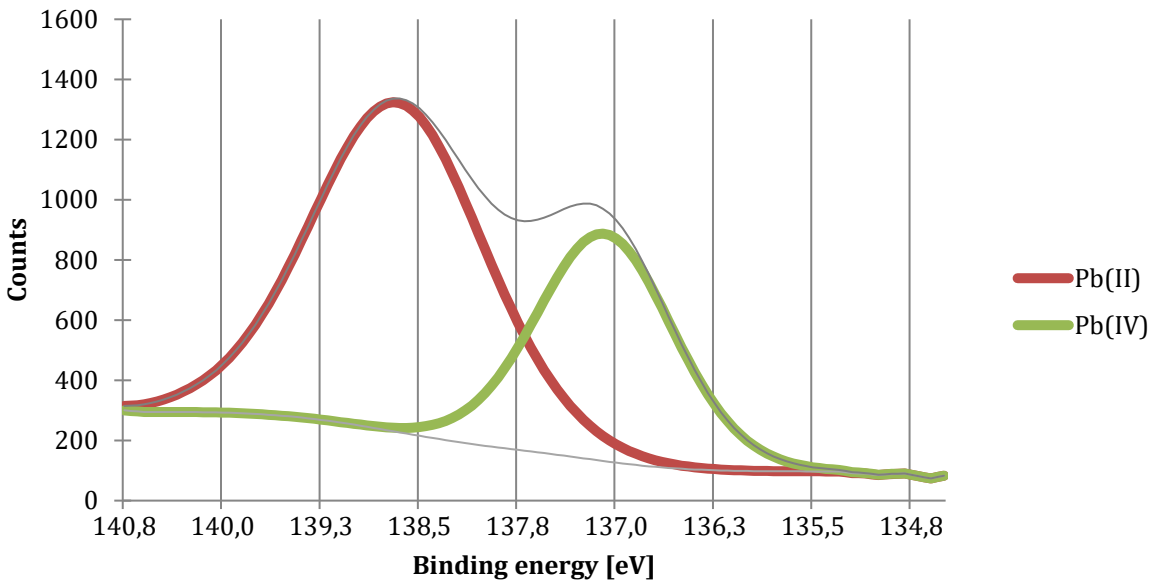

Figure 4.2: Pb 4f region scan of the LBP coating after 5s sputtering. Sample 3.

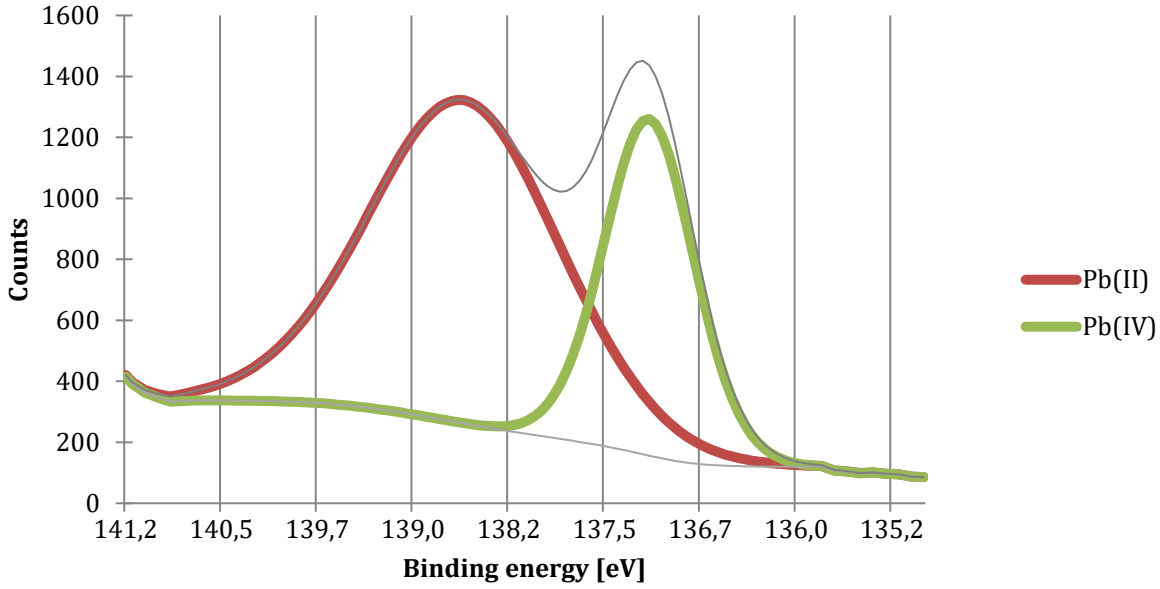

Figure 4.3: Pb 4f region scan of the LBP coating after 15s sputtering. Sample 3.

Figure 4.4, 4.5 and 4.6 shows the results from the regional scans for Pb 4f of the steel surface (Sample 2) after 0, 5 and 15 seconds sputtering time respectively. After 0s sputtering, one distinctive peak is found at 138.8eV. For 5s and 15s sputtering two peaks are found at 138.6eV and 136.8eV. The peak at 138.6eV is assumed to be Pb(II), referring to Figure 4.2 and 4.3. The peak located at 136.8eV is assumed to be metallic lead since it is shifted 0.3eV compared to Pb(IV) and previous papers support that this peak represents metallic lead [32, 33]. The atomic percentage of metallic lead (relative to the total amount of lead) is 5at% and 16at% for 5s and 15s of sputtering time.

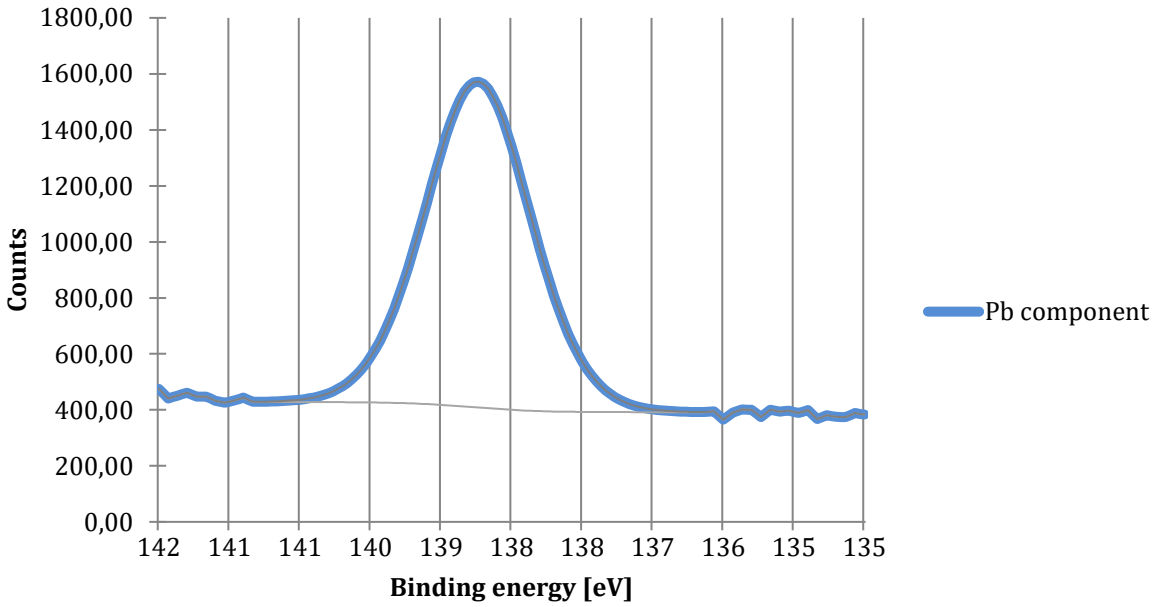

Figure 4.4: Pb 4f region scan of the steel surface after 0s sputtering. Sample 2.

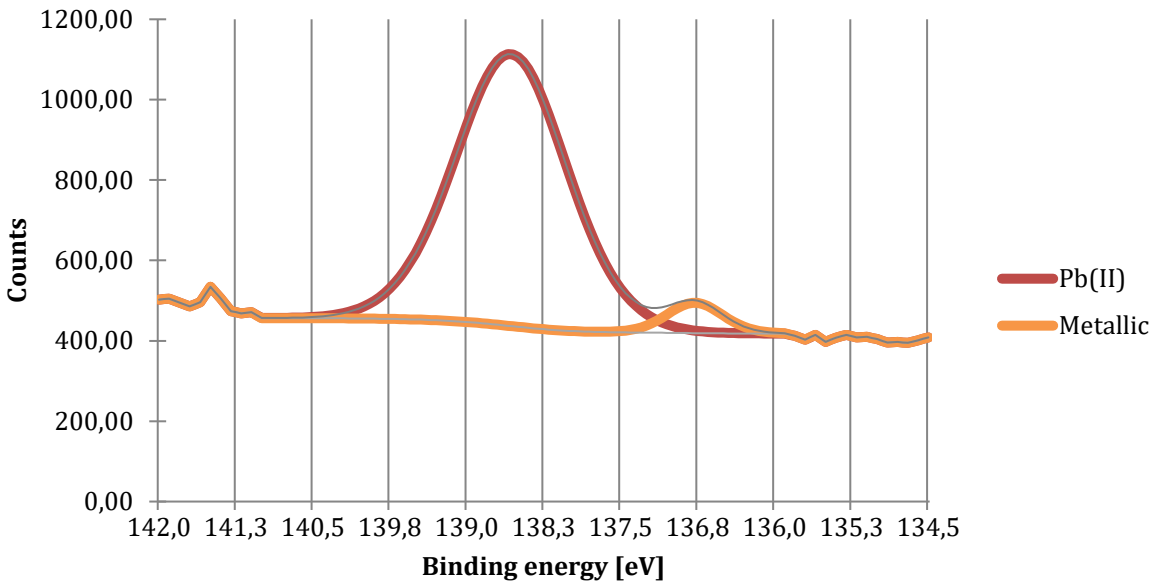

Figure 4.5: Pb 4f region scan of the steel surface after 5s sputtering. Sample 2.

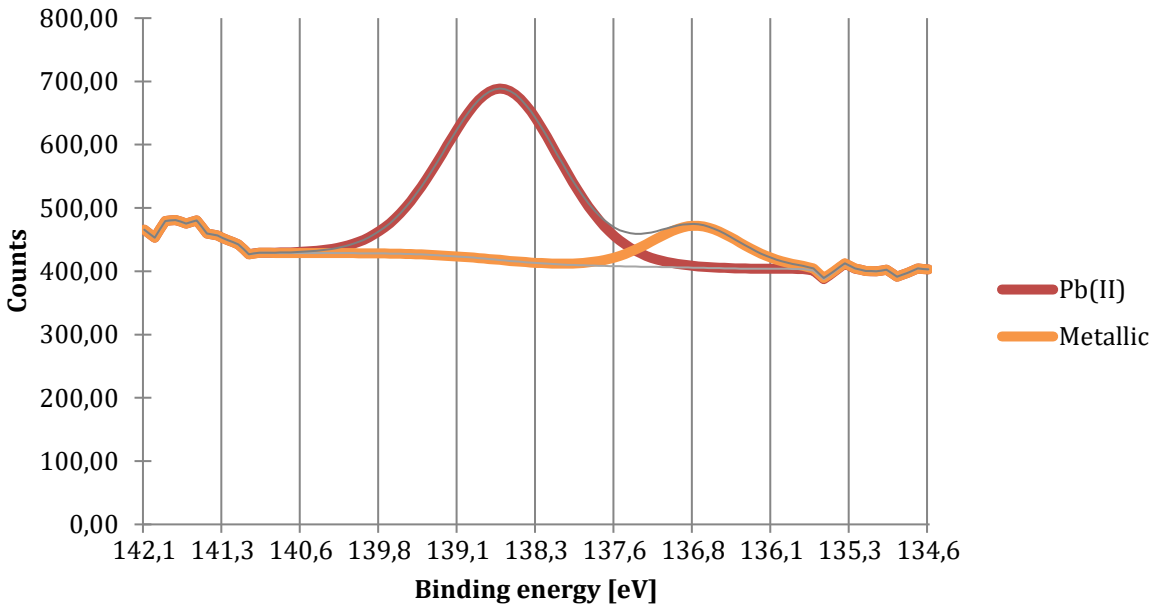

Figure 4.6: Pb 4f region scan of the steel surface after 15s sputtering. Sample 2.

Table 4.1 shows the relative atomic concentration of lead against iron, carbon and oxygen. At greater depths than after 15 seconds with sputtering, the traces of lead were too small to be considered as a significant result. Figure 4.7 shows lead, iron, carbon and oxygen in comparison to each other.

Table 4.1: Atomic percentage of lead from survey scans.

Sputtering time (s)	Relative atomic percentage, Sample 2 (%)
0	2.22
5	1.93
15	1.11
115	0.31
615	0.00

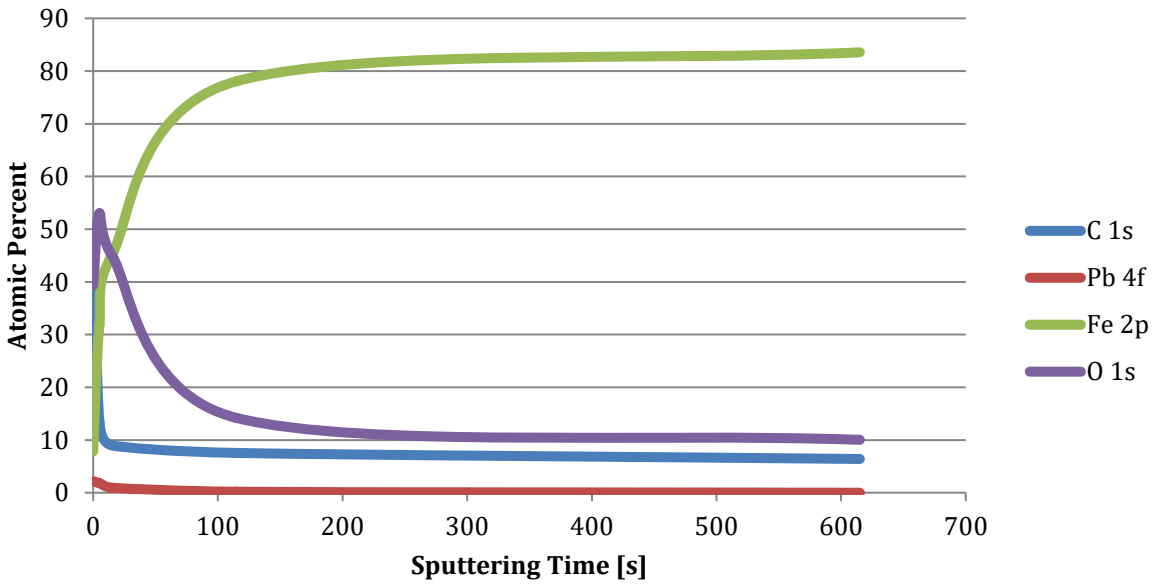

Figure 4.7: Atomic percentage of elements of interest at different sputtering times. Sample 2.

Figure 4.8 show the relative concentration of different iron species trough the iron oxide. From 200 seconds with sputtering to 615 seconds, it is not noticed any difference between the species. This part of the depth profile is therefore removed. Figure 4.9 is only showing the oxides from Figure 4.8, while Figure 4.10 is only showing the metallic iron. It can be seen that LBP (Sample 2) does not give a thicker oxide compared to the surface painted with epoxy or the bare steel surface. If anything, the steel painted with red lead shows a higher content of metallic iron. The quantity of metallic iron is higher for LBP (Figure 4.10) and the quantity of iron oxide species is also lower for LBP (Figure 4.9). The bare steel surface (Sample 1) and the surface under epoxy (Sample 4) can be described as close to identical in terms of metallic iron, as seen in figure 4.10.

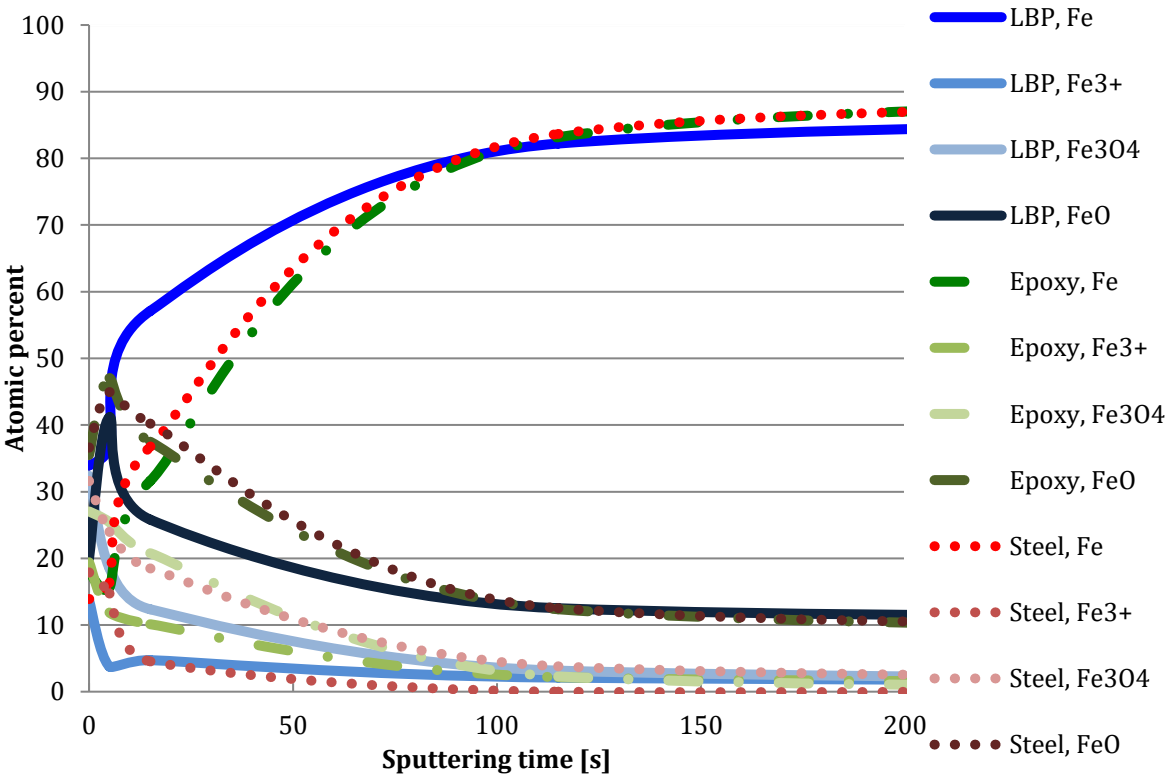

Figure 4.8: The relative concentration of different iron species trough the iron oxide under LBP (Sample 2) and epoxy (Sample 4) and for the bare steel (Sample 1).

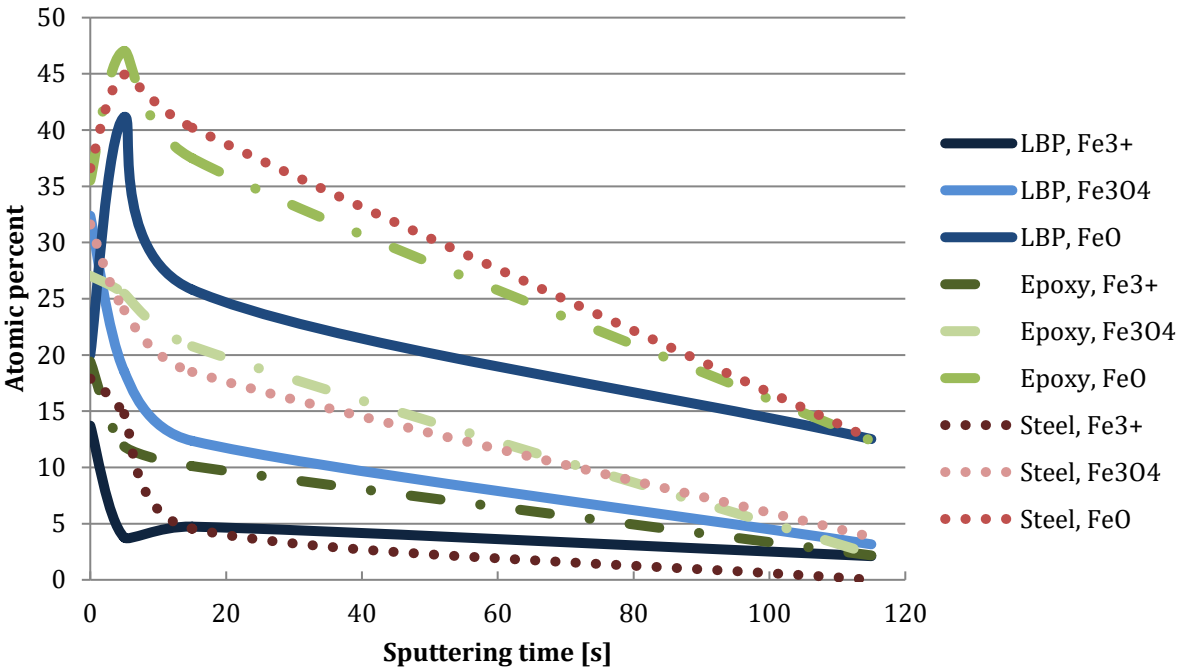

Figure 4.9: The relative concentration of different iron species, down to 115 seconds sputtering. Scan from Sample 1 (Steel), Sample 2 (LBP), and Sample 4 (Epoxy).

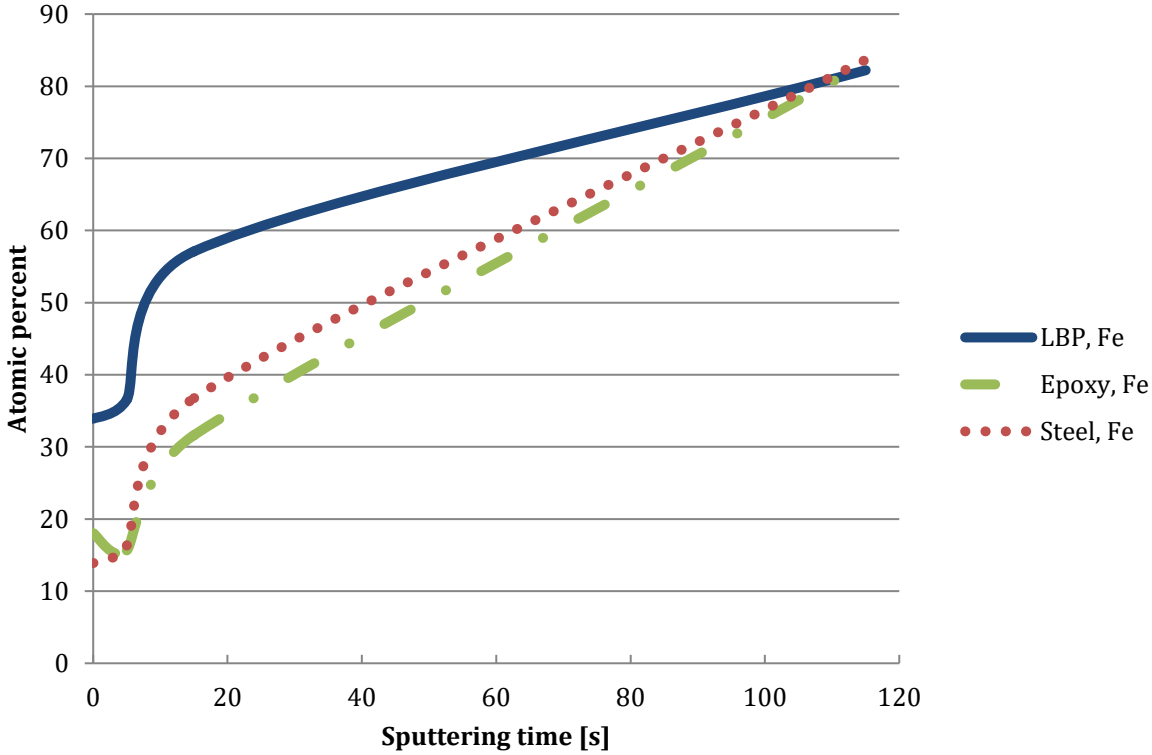

Figure 4.10: The relative concentration of metallic iron, down to 115 seconds sputtering. Scan from Sample 1 (Steel), Sample 2 (LBP), and Sample 4 (Epoxy).

4.2 Transmission Electron Microscopy

Figure 4.11 shows a TEM picture over the cross-section of the LBP, oxide, and steel. The EDS/EELS analysis was performed in the blue (20nm) and yellow (5nm) marked area. Both areas consist of a thin oxide between the steel and the paint. The results from the EDS/EELS analysis are shown in Figure 4.12, and in Figure 4.13 at a higher resolution. A mapping of Fe, O and Pb is displayed. Other materials, such as C, Si, P, Cr and Mn are found in the oxide, while Ni and As was found, additional to previous mention elements, in the bulk material. Only small quantities of lead are found in the oxide, and as seen in Figure 4.12e and 4.13e lead is segregated in lower parts of the iron oxide.

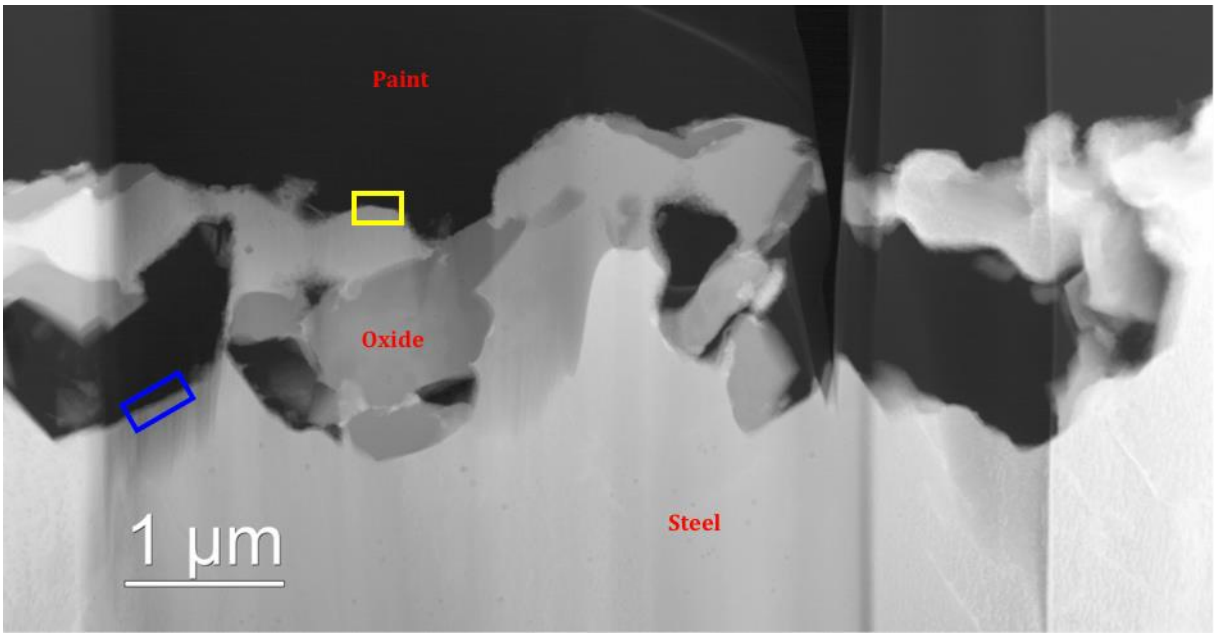

Figure 4.11: TEM picture of the cross-section of the bridge sample. Showing steel, oxide and paint. The blue and yellow markings are the area for EDS/EELS analysis.

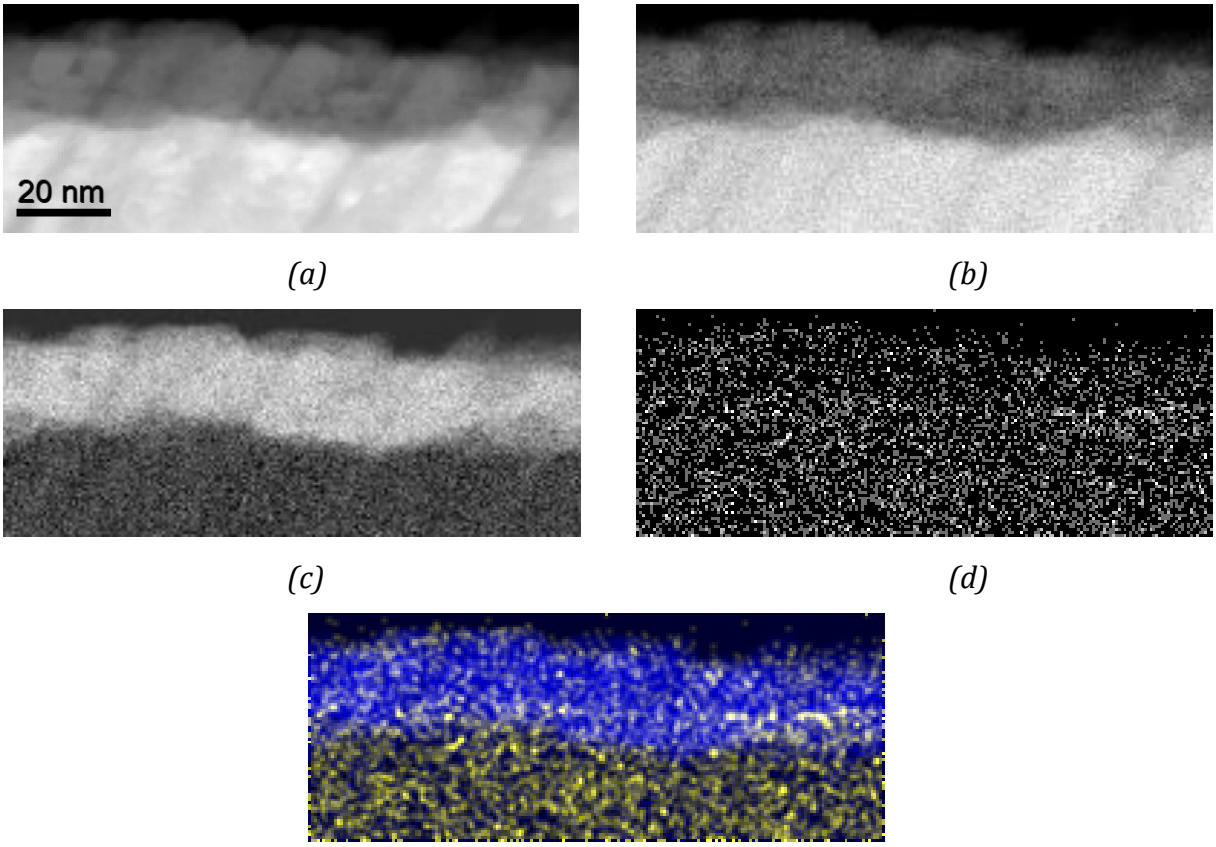

(a) *(b)*

(c) *(d)*

(e)

Figure 4.12: 20nm STEM picture (a), EELS scan of Fe (b), EELS scan of O (c), EDS scan of Pb (d), EELS of O + EDS, filtered of Pb (e). Oxygen in blue and lead in yellow.

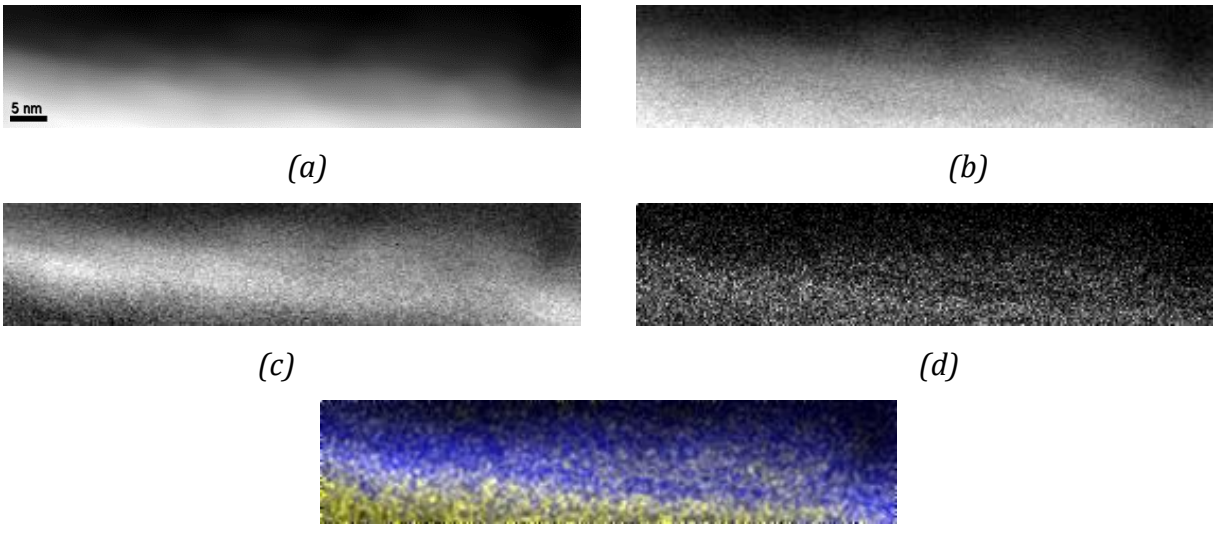

(a) *(b)*

(c) *(d)*

(e)

Figure 4.13: 5nm STEM picture (a), EELS scan of Fe (b), EELS scan of O (c), EDS scan of Pb (d), EELS of O + EDS, filtered of Pb (e). Oxygen in blue and lead in yellow.

4.3 Scanning Kelvin Probe

4.3.1 Point measurements

Figure 4.14 shows the results of the point measurement of the coating and the bare steel, before the introduction of a reservoir. As it is seen the potential of bare steel is found in the range between 230mV to 330mV, which is in good agreement with the reported potential of steel exposed to air [34]. The potential of protected steel under the LBP coating is found to range from 0mV to 150mV. The steel surface is passivated under the paint.

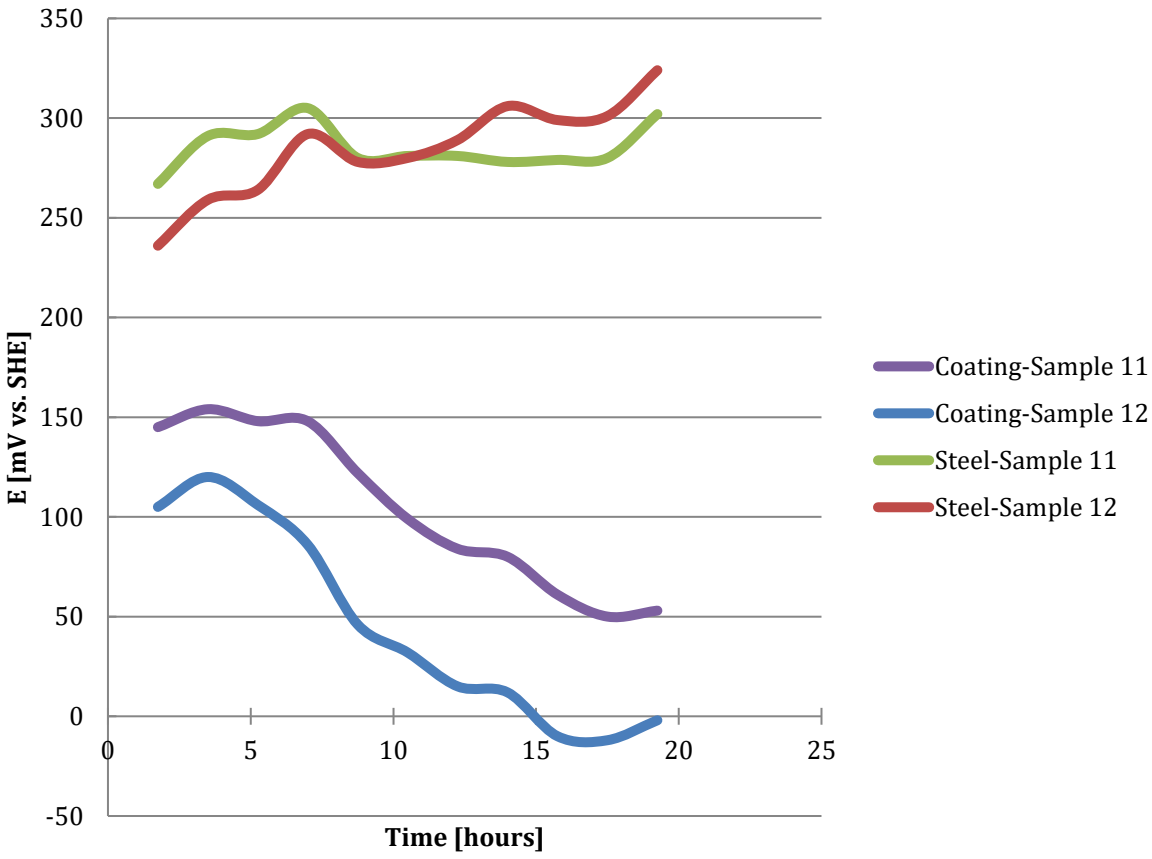

Figure 4.14: Point measurements of Sample 11 and 12 over the coating (LBP) and the bare steel. The time is referring to hours after insertion of the samples into the test chamber.

4.3.2 Catodic Disbonding Test

Figure 4.15 shows the potential over the NaCl reservoir. The potential is stable at around -0.5V vs. SHEfor both Sample 11 and 12, which is close to the theoretical equilibrium potential of iron at -0.44V vs. SHE[13].

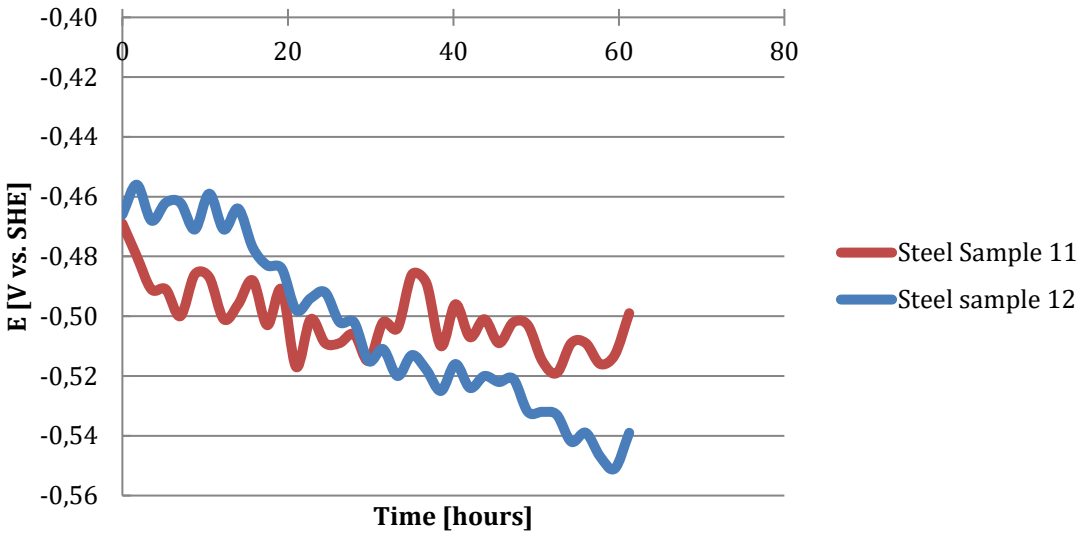

Figure 4.15: Potential measurements over the NaCl reservoir. The time is referring to hours after insertion of the reservoir.

Figure 4.16 and 4.17 shows the CD sweeps of Sample 11 and 12 during the first test round (the paint has cured for two days). In both figures it is seen that the potential is falling before it stabilised at a potential around -0.220V to -0.270V. The potential decreased over the whole length of the scan, and the characteristic delamination front for CD tests (A rapid increase in potential. From a low potential at areas with damaged coating to a higher potential at areas with un-damaged coating) was not observed.

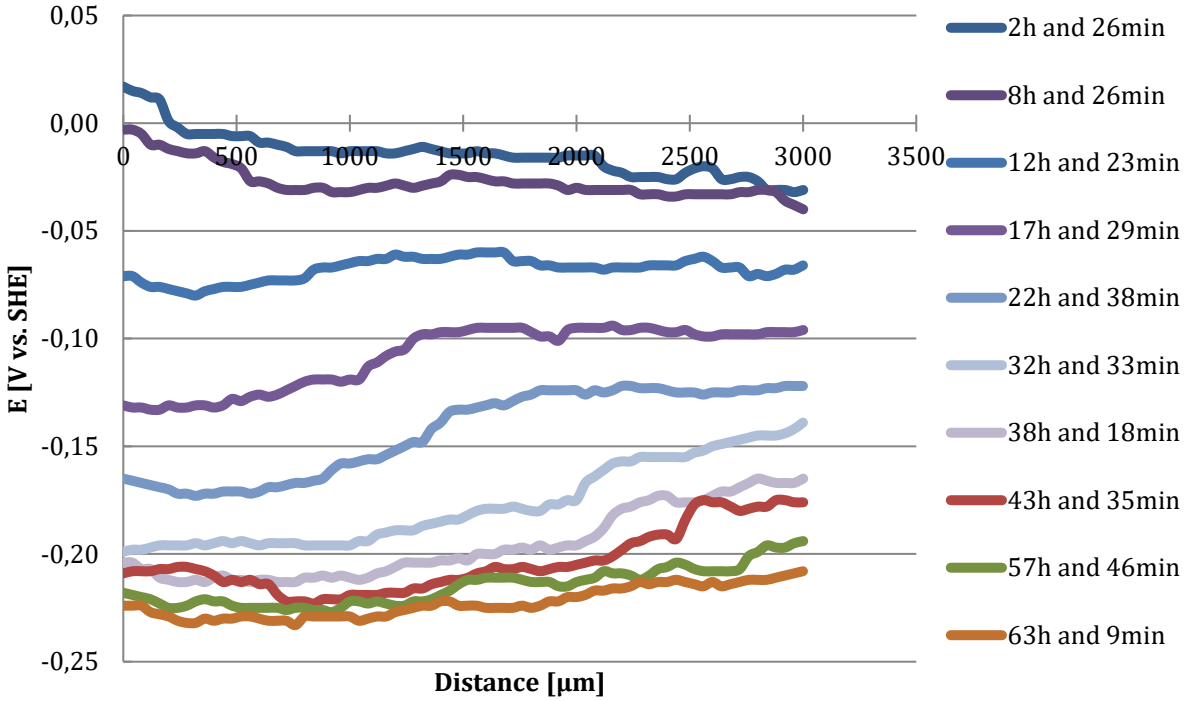

Figure 4.16: CD test of Sample 11. First test round. The time is referring to hours after insertion of the reservoir.

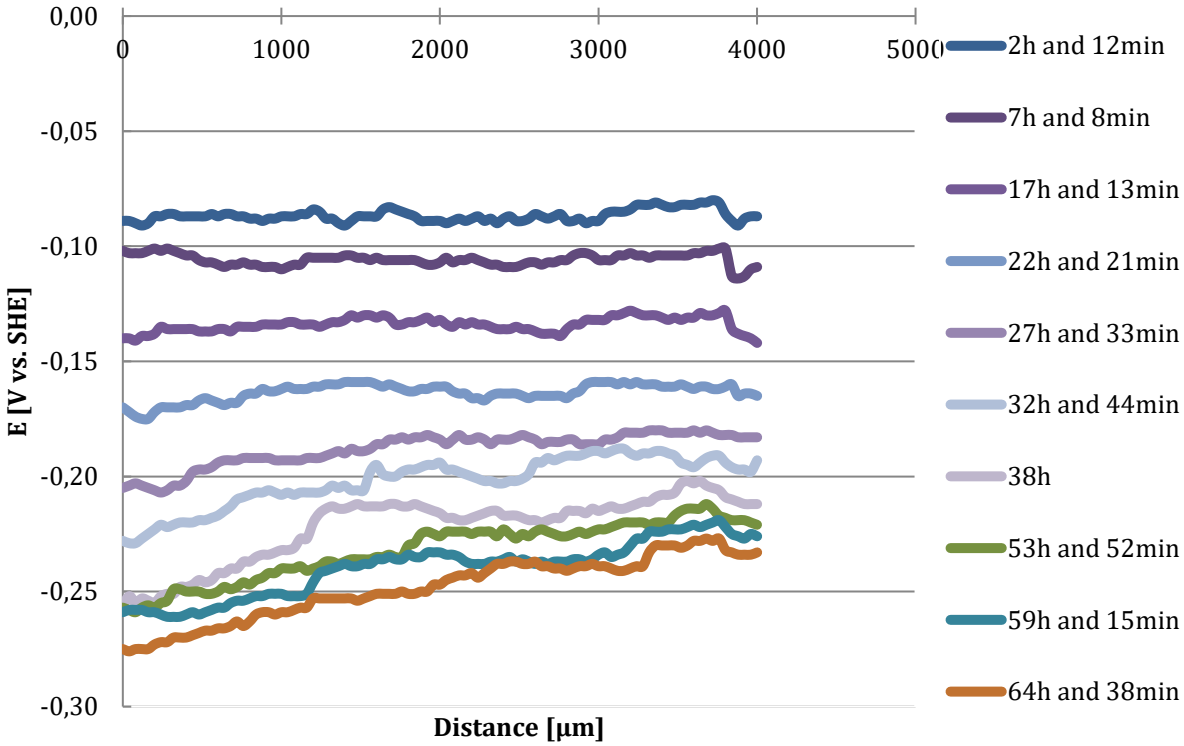

Figure 4.17: CD test of Sample 12. First test round. The time is referring to hours after inserting the reservoir.

Figure 4.18 and 4.19 show the scan over the coating (Sample 11 and 13) before the reservoir is introduced during the second test round (The paint has cured for weeks). Sample 13 has a potential 150mV vs. SHE when steel is protected under the LBP, which matches the potential measured during the point measurements before the first CD test round (Figure 4.14). For Sample 11 the potential is -150mV vs. SHE. The thickness of the coating will affect the potential for passivation of the steel surface. To make sure the potential measurements was done over a distance with constant thickness and hence potential, the scan length shown in Figure 4.18 is from 1500µm to 5000µm. The whole scan length is shown in Appendix B, which include discussion for the potential variation.

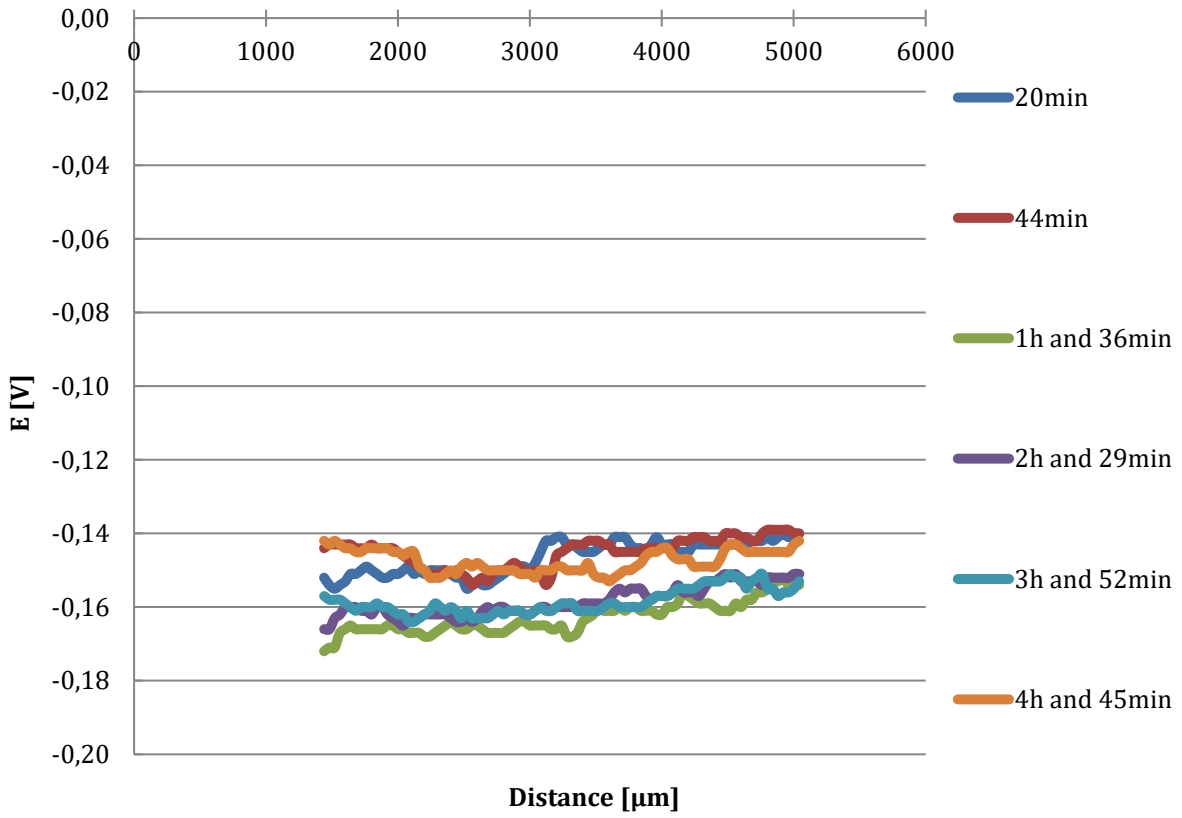

Figure 4.18: Measured potential prior to the CD test of Sample 11. The time is referring to hours after insertion of the samples into the test chamber.

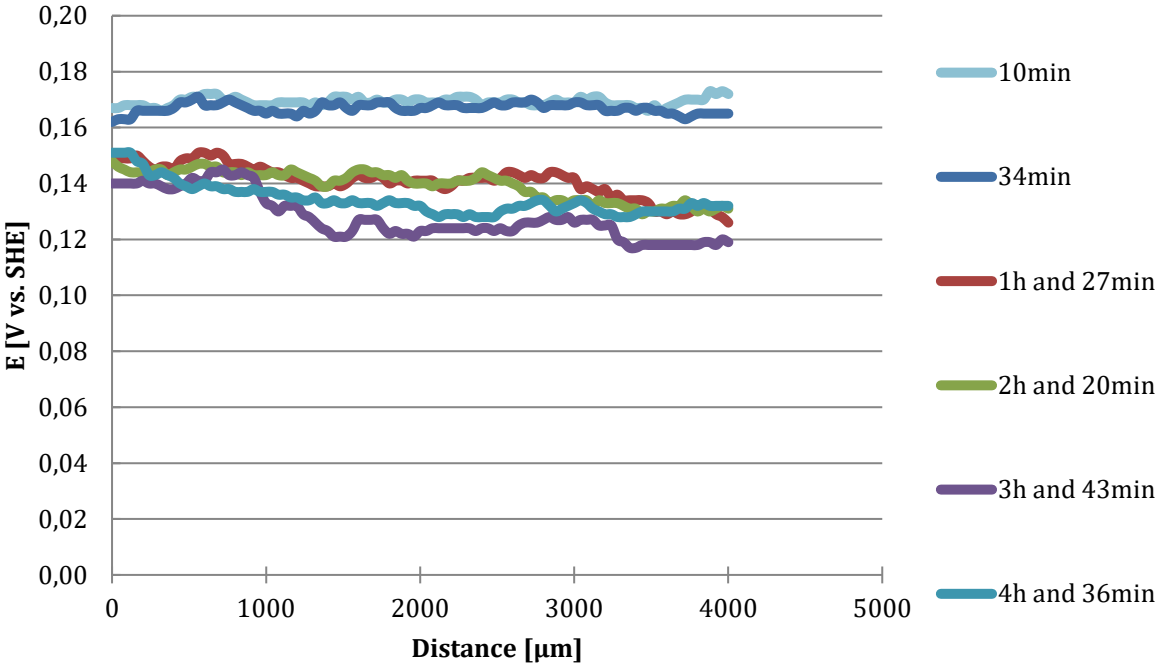

Figure 4.19: Measured potential prior to the CD test of Sample 13. The time is referring to hours after insertion of the samples into the test chamber.

The result of the second test round is shown in Figure 4.20 and 4.21 for Sample 11 and 13. Figure 4.20 shows the results between 1500µm from the reservoir, to 5000µm. As seen from Figure 4.20 the initial measurements showed similar behaviour as the pre-scan (Figure 4.18). Subsequently the potential measured 5000µm away from the reservoir increased to between -0.08V and -0.02V vs. SHE, which is higher than the potential measured in the pre-scan. Close to the reservoir (near the damage), it is observed a drop in potential to, but not under, -0.220V vs. SHE. The same effect is seen for the damaged areas on Sample 13 (Figure 4.21). The potential does not drop under -0.225V vs. SHE. For this sample, the un-damaged coating (furthers away from the reservoir) stabilises at a potential level similar to the pre-scan (Figure 4.19). No increase in potential is observed at this area.

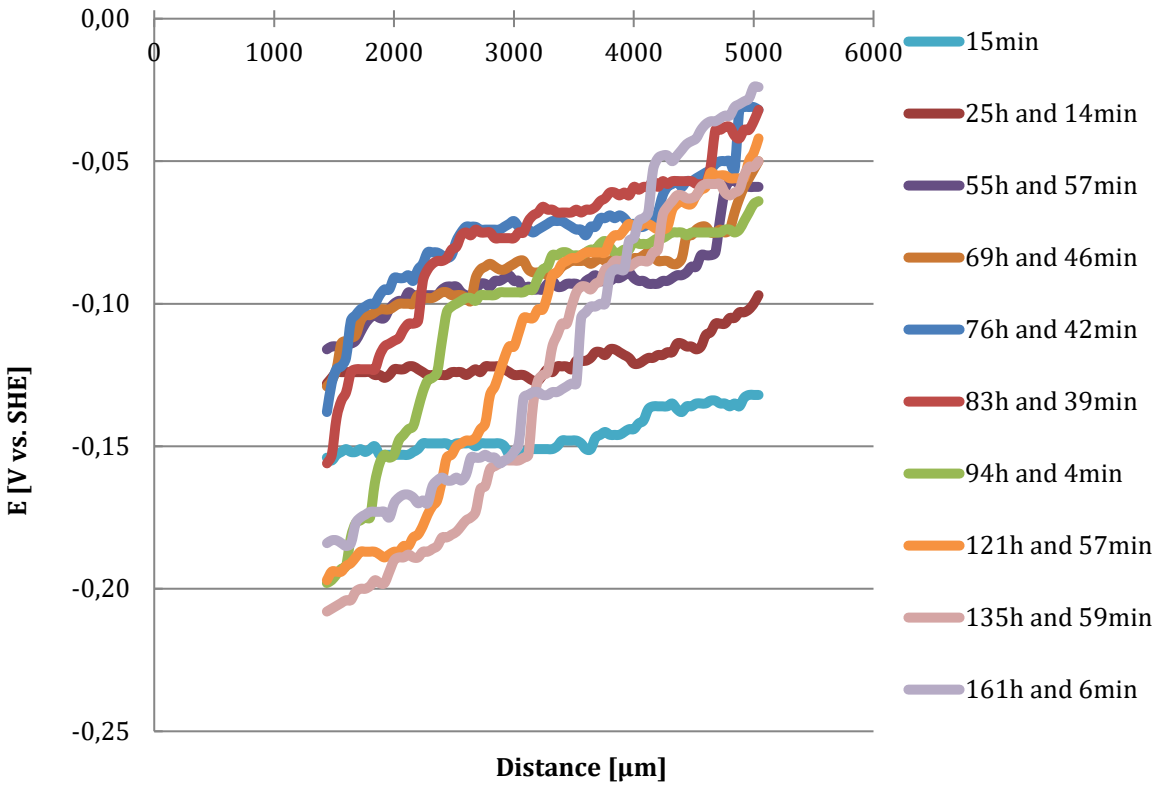

Figure 4.20: CD test of Sample 11. Second test round. The time is referring to hours after insertion of the reservoir.

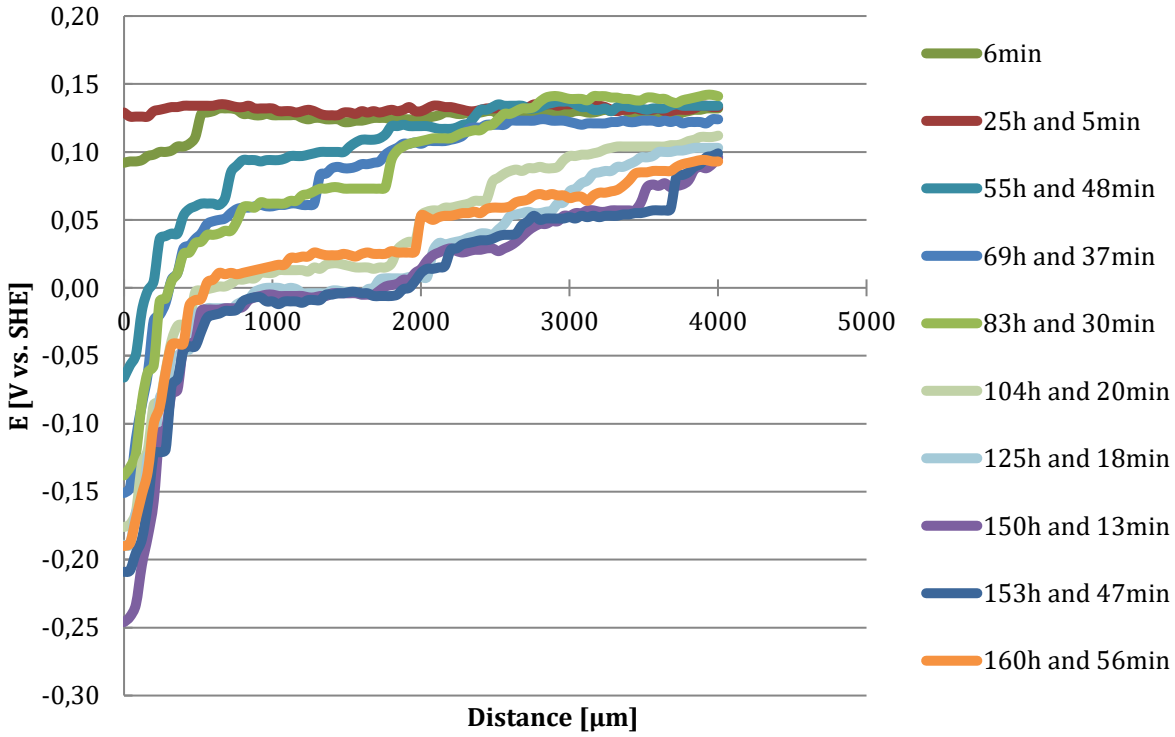

Figure 4.21: CD test of Sample 13. Second test round. The time is referring to hours after insertion of the reservoir.

4.3 X-Ray Diffraction

XRD was performed in an attempt to compere with the results found by Vetere and Romagnoli [30]. Figure 4.22 shows the XRD scan for the 2θ region from15° to 65° of Sample 1 and 2. As the figure shows the sample consists mainly of iron (marked with the red dot, Figure 4.22). Figure 4.23 and 4.24 shows peaks found at lower intensities. Three peaks are found in Sample 2 (blue curve), while none is found in Sample 1 (red curve). The peak marked with a black dot is a reflection of the Cu Kα source and can be seen in both of the samples. The three peaks can be identified as lead components, but it is difficult to determine what kind of component. Two (green dots) of the peaks could be from red lead, while the last peak (orange) could originate from either PbO (massicot) or metallic Pb. However, since the intensity is too low (no repetitive peaks are observed), it is not possible to conclude about which kind of lead components are present. The reference for the different iron and lead species is taken from International Centre for Diffraction Date and has the following PDF number: Fe: PDF 00-006-0696, Pb_3O_4: PDF 00-041-1493, Pb: PDF 00-044-0872, PbO: PDF 04-013-9603, $PbFe_4O_7$: PDF 00-022-0656[35].

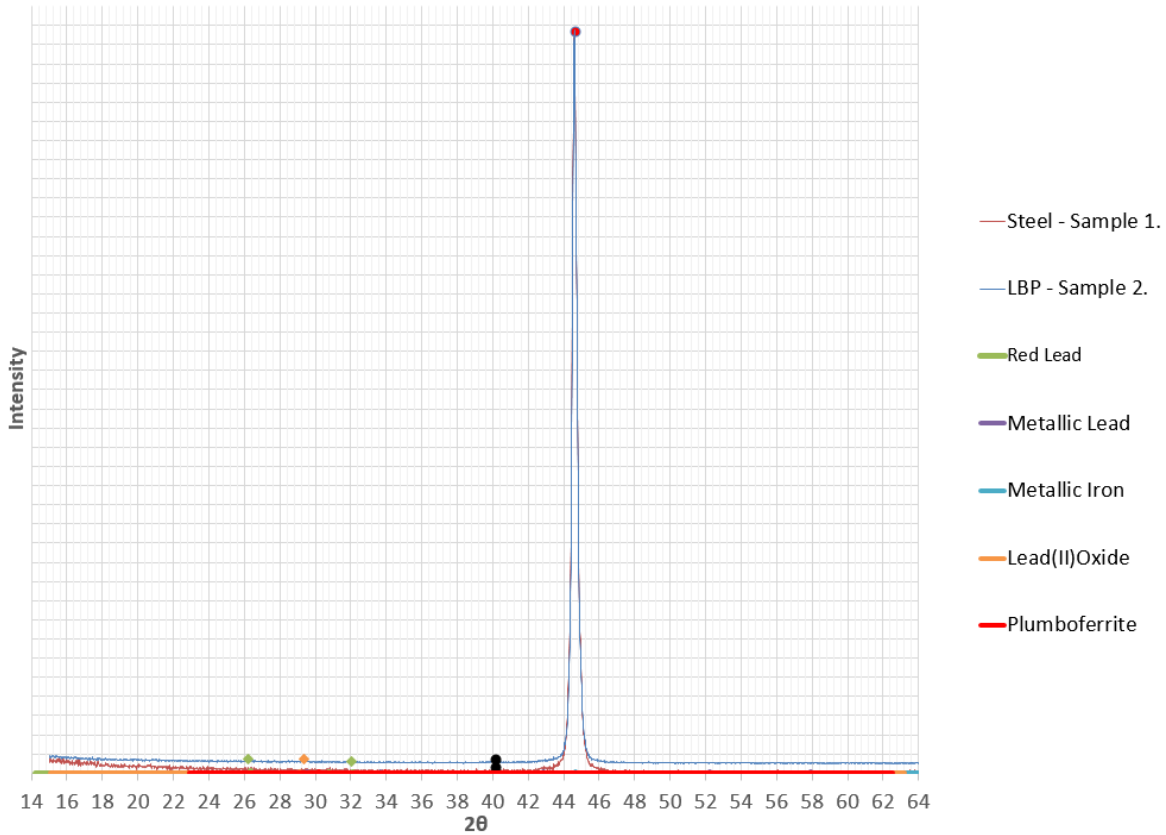

Figure 4.22: XRD scan of the surface of Sample 1 and 2. 2θ from 15° to 64°.

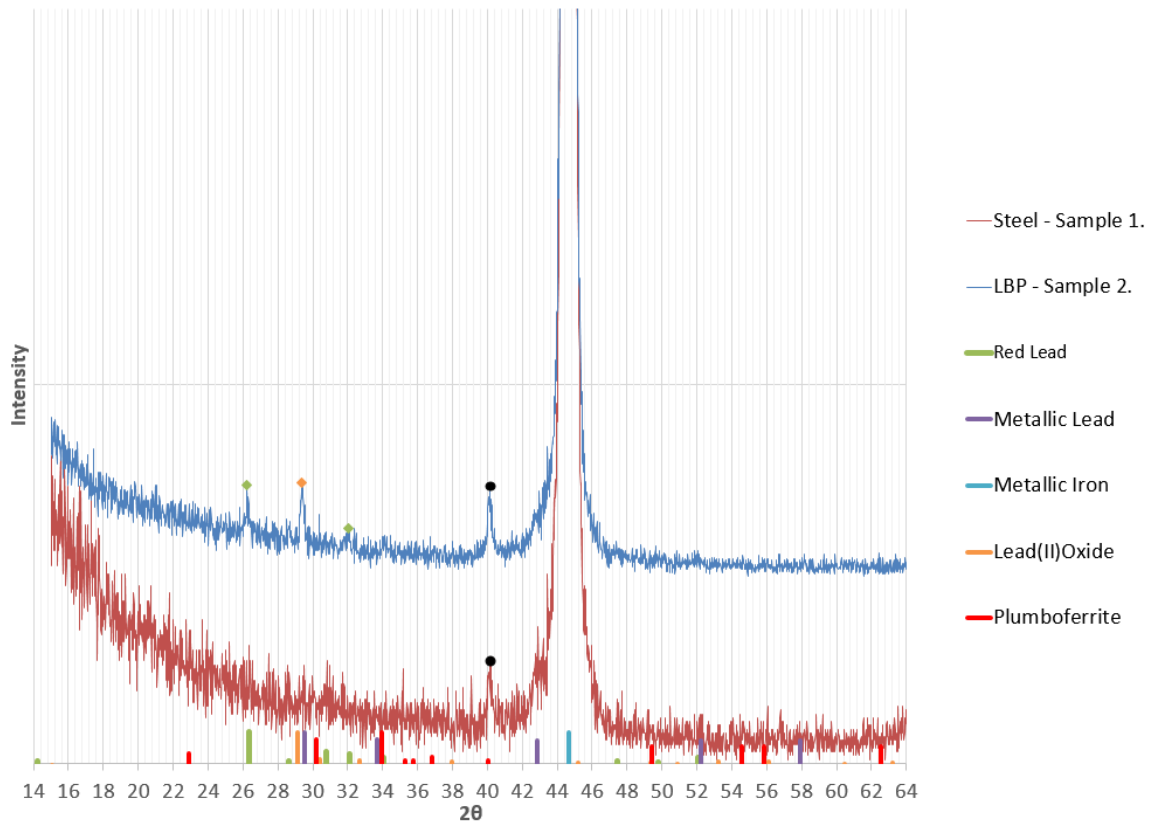

Figure 4.23: XRD scan of the surface of Sample 1 and 2, low intensity. 2θ from 15° to 64°.

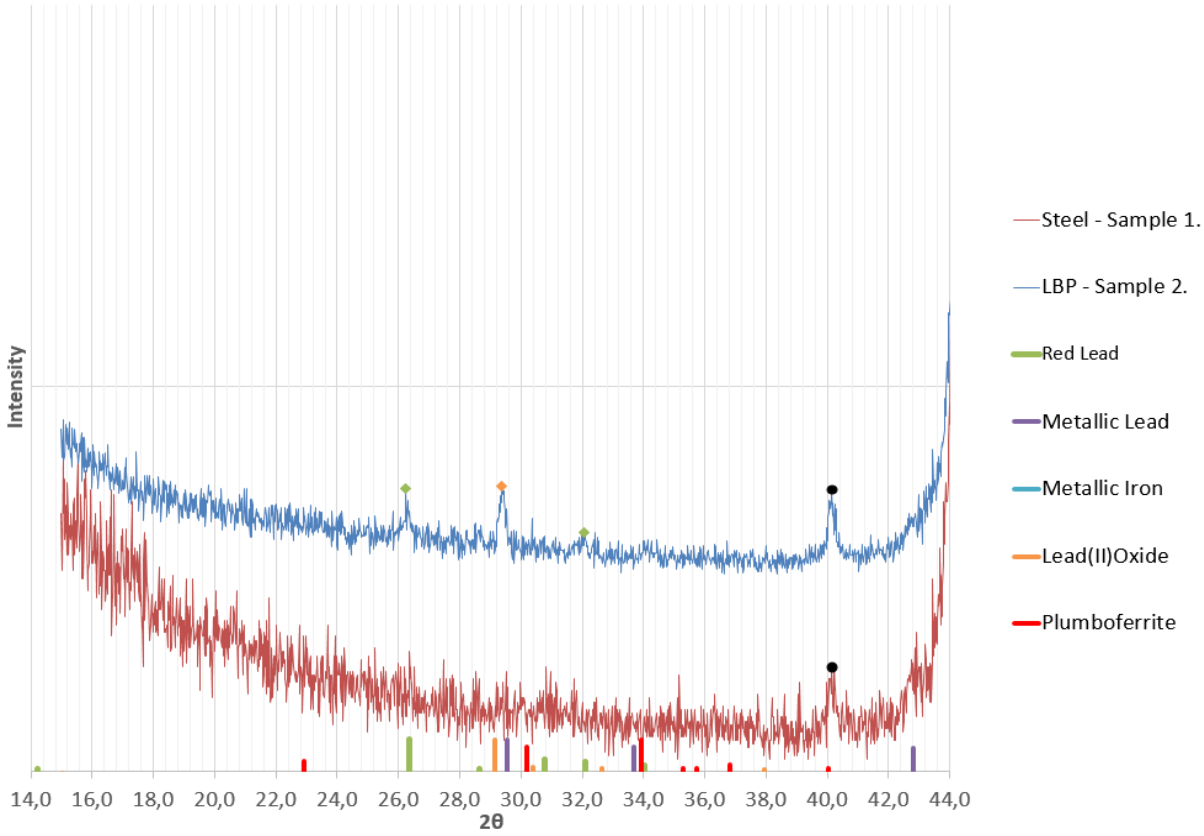

Figure 4.24: XRD scan of the surface of Sample 1 and 2, low intensity. 2θ from 15° to 44°.

5. Discussion

5.1 X-Ray Photoelectron Spectrometry

Figure 4.2 and 4.3 shows that the red lead pigment in the paint act as a useful reference for the investigation of the lead oxides. The clear 2:1 ratio between lead(II)oxide and lead(IV)oxide is shown in the results as a PbO peak at 138.6eV while PbO_2 is found at 137.1eV. This ratio between PbO and PbO_2 is in good agreement with the known structure of red lead, as explained in section 2.3.2. Reported values for different lead oxide peaks are overlapping and varies a lot in the literature [33]. However, PbO is usually found at higher energies than PbO_2 [33, 36] and similar results with a dual peak for Pb_3O_4 is previously reported [31].

From the XPS results of the surface oxide under the LBP (Sample 2, Figure 4.4) shows that lead is present as a lead component found at 138.8eV, which is close to the reported value for PbO. Since it is only shifted 0.2eV from the reference it is likely that this species is some salt of Pb^{2+}, e.g. lead hydroxide or lead carbonate. Lead hydroxide is closely related to PbO, as seen in Figure 2.2 and 2.3. Interestingly, only one single peak at 138.9eV is observed in the top layer of the LBP (Figure 4.1, Sample 3). This result will be discussed further in subsection 5.5.

Further down in the surface oxide the main lead peak is shifted back to 138.6eV (Figure 4.5 and 4.6). More interesting on this depth is the presence of a new peak located at 136.8eV. This peak is likely to be metallic lead since the theory is quite clear that the metallic lead peak is located [33]. It can be argued that since the peak is only shifted by 0.3eV it could be traces of a Pb^{4+} species, but PbO_2 needs to be a product of a strong oxidation process, which is unlikely. Especially since steel, which is anodic to lead in most cases, probably will polarise the sample to a too low potential. The observed quantity of 5at% and 16at% (relative to total amount of lead elements) at 5 and 15 seconds sputtering time (Figure 4.5 and 4.6) shows that the 2:1 ratio, as seen in the LBP coating (Figure 4.2 and 4.3), is not present. Therefore, the ratio between the reported lead peaks indicates that this species is not red lead, which could have been absorbed.

It seems reasonable to assume that the lead present at the surface of the oxide is a lead(II) component, while deeper down in the oxide the lead is present as mainly PbO, but also some metallic lead.

No indication of a thickness growth in the surface oxide is observed by looking at the iron concentration depth profile. If anything, it could seem like the reference samples have a thicker oxide, i.e. that the absorption of lead into the surface oxide makes it thinner.

5.2 Scanning Kelvin Probe

The most significant SKP results are that the corrosion potential under the damage in the coating, during CD tests, does not fall below -0.225 to -0.270 V vs. SHE for any of the tested samples. This potential is considerably higher than the theoretical equilibrium potential of steel at -0.44V vs. SHE. The measured potential of -0.50V vs. SHE over the NaCl reservoir, as shown in Figure 4.15, is close to the theoretical equilibrium potential of iron as expected [37-39].

Over the bare steel exposed to air, the potential was measured to 250-300mV vs. SHE (Figure 4.14), which is according to previously reported values [34]. The passivation potential for the steel surface under the LBP is measured from 0V vs. SHE to 0.15V vs. SHE for Sample 11, 12 and 13(as shown in Figure 4.14 and 4.19). No previous reference is found in the literature for the passivation potential of steel under LBP. Interestingly, for Sample 11 this potential has dropped to -0.15V vs. SHE before the second CD test (Figure 4.18). Different explanations for the drop in the observed potential are possible. The thickness of the coating may explain the potential drop. As seen from Appendix B, the potential varies with the thickness of the coating. Another explanation can be due to the fact that the sample was conditioned before the second test. The argument is that the negative measured passivation potential is only observed for Sample 11, which is the only sample that has been previously exposed to a humid environment.

During the first CD test, it was seen that the potential decreased along the entire scanned distance. A possible explanation for this observation could be that the paint does not provide a good enough barrier protection against migration of water. Alkyd paint is a one-component paint, which cures slowly. A curing time of two days before exposure did not seem to be sufficient in regards to adhesion and barrier properties. A similar effect (stabile measured potential over the whole scan distance) is seen in the initial period of the second CD test (Figure 4.20 and 4.21), but this effect is probably due to a lack of an electrolyte. In other words, it could be that it will take some time from the introduction of the reservoir to the establishment of an effective electrolyte and thereby an effective corrosion cell. This potential is equivalent to the measured potential before addition of electrolyte to the reservoir (Figure 4.18 and 4.19).

Another interesting observation from the SKP test is the potential increase at the passivated sites (beyond the disbanding front) as seen in Figure 4.20. The potential over the un-damaged coating increased to -0.06V vs. SHE (Figure 4.20) from the initially measured potential between -0.14V and -0.17V vs. SHE(Figure 4.18). This observation could be due to the establishment of a galvanic cell as previously explained, but it could also be due to an unknown reason.

5.3 Transmission Electron Microscopy and X-Ray Diffraction

The concentration of lead in the surface oxide was not high enough to enable characterisation of the oxidation state of the lead species with the use of XRD. However, it is possible to conclude that lead is present in the outer surface of the sample, and it strengthens the argument that corrosion protection by LBP is due to the presence of lead on the steel surface. It can be concluded that the sample preparation during this thesis is not suited for XRD, since lead is only present in the top oxide. Therefore, it is not possible to compare the results to the XRD test performed by Vetere and Romagnoli[30].

The EDS/EELS results in TEM showed that lead was present only in small quantities and was segregated to the lower parts of the iron oxide (close to the metal/oxide interface). The anodic sites in a corrosion cell are located close to the bulk surface, while cathodic sites are located on the top of the surface oxide. However, the lead may also originate from the bulk metal since the sample was taken from an unknown steel grade from a bridge. But assuming that the lead originated from the paint, it will be in agreement with theories that believe that lead is deposited at anodic sites. However, this is contradictory to the observed concentrations of lead during XPS analysis, which showed a decreasing lead concentration at deeper oxide depths.

5.4 Deposition and Protection Mechanism

It has on several occasions been proven that the electrolyte will contain ionic lead, either dissolved as lead azelate and/or directly solved from the pigment. Mayne et al. [20] have summarised three different deposition mechanism, which in terms can provide important information about the true protection mechanism of LBP. They are as follows:

- Deposition due to precipitation of lead cations. Most likely $Pb(OH)_2$ / PbO.
- Deposition of plumbate/plumbite anions, e.g. PbO_4^{4-} / PbO_2^{2-}.
- Cathodic deposition of metallic lead.

The XPS results showed mostly PbO in the surface oxide, but further down in the oxide metallic lead was found in increasing quantities. The SKP examination shows that the corrosion potential of steel was about -0.25V vs. SHE. It appears that this potential can be related to the inhibition of corrosion on the steel.

A potential of -0.25V vs. SHE corresponds to the potential for cathodic deposition of metallic lead if the molar concentration of ionic lead is in the 10^{-4} order, according to Eq. 1. However, it is also the concentration for precipitation of lead(II)oxide or lead hydroxide at a pH ≈ 8.3, according to Eq. 3. Mickalonis and Leidheiser [16] have reported a corrosion potential of -500mV vs. SCE (-256mV vs. SHE) at a lead concentration of 10^{-3}M and pH = 4.5 (Figure 2.5), which is close to the measured potential from the SKP test. At this pH, the solubility of PbO is too high for precipitation of lead(II)oxide from the electrolyte, and it is therefore likely that the deposited lead is metallic.

If cathodic deposition of metallic lead is occurring, it has to somehow oxidise to PbO. The majority of the lead present in the surface oxide is lead(II)oxide. Lindqvist [28] observed that the lead acted as anode against steel for some hours before it turned back to being the cathode. A possible reaction where the lead will be anodic to steel is given in Eq. 4. This reaction requires access to OH^-, which is known to be formed at cathodic sites at steel due to oxygen reduction.

If the corrosion protection is a result of precipitation of $PbO/Pb(OH)_2$ it must be assumed that the lead oxide improves the protective properties of the surface oxide. If the lead is deposited as lead oxide, a problem that must be answered is why metallic lead is present at the surface. In most cases lead is cathodic to steel, and a galvanic cell can result in the formation of metallic lead. With the potential seen in the SKP, Eq 2 could be a possible explanation of the formation of metallic lead. If Eq 2 is solved for a pH = 4.5, the equilibrium potential will be E_0 = -0.018V, which deviates from the corrosion potential observed by Mickalonis and Leidheiser [16] as shown in Figure 2.5. The corrosion potential measured by SKP will give a pH of around 8.0 if the reaction in Eq. 2 occurs, which could be a imaginable pH for this system.

The last proposed mechanism is the deposition of plumbate/plumbite. As explained by Mayne et al. [20] the quantities of plumbate in equilibrium with 10^{-4}M Pb^{+} is in practice infinitive small. As seen in the Poubaix diagram for lead (Figure 2.2 and 2.3), plumbate in the electrolyte is most likely in alkaline conditions.

To summarise it seems like that the most likely deposition mechanism is cathodic deposition of metallic lead from ionic lead in the electrolyte. The main argument for this is that metallic lead is observed in XPS. Besides, the SKP test shows that the potential does not drop below a potential -0.25V vs. SHE. However, deposition of PbO could occur at this potential, but in a limited pH range. The previous literature has described inhibition of steel surfaces in contact with lead oxide and/or metallic lead over a wide range of pH [16, 17, 22, 27]. Precipitation deposition is not potential dependent, as it known from the vertical lines in the Pourboix diagram. Therefore, it is likely that the deposition of lead is due to cathodic deposition.

If it is accepted that inhibition of corrosion is due to the deposition of metallic lead at the surface, three mechanisms seem to be possible:

- A healing or even a growth of protective iron oxide due to depolarisation of reduction reaction. By healing it is meant a repair of weak spots in the oxide where formation of *iron oxide* provides better resistance against anodic dissolution of the steel and/or the cathodic reaction on the steel. This is anodic protection.
- A strengthening of the protective oxide is due to the presence of lead oxide in the iron oxide matrix. The *lead oxide* will provide a film with higher resistance against anodic dissolution of the steel and/or cathodic reduction.
- A barrier effect is locally achieved. The *metallic lead* could hinder anodic dissolution of the steel and/or slow down the cathodic reaction.

Previous theories that have supported cathodic deposition of metallic lead, believe in a growth or healing of the iron oxide [16, 20, 28]. This mechanism is explained by depolarisation of the oxygen reaction, which provides sufficient current on the steel to move the potential into passivation. In other words, this depolarisation leads to anodic protection of the steel. Since deposition of metallic lead is occurring the total cathodic current has to increase and hence anodic current has to increase, which could be sufficient to polarise the steel surface into a passive state.

Another proposed protection mechanism is a strengthening of the surface oxide matrix due to the presence of lead oxide. Vetere and Romagnoli [30] proposed that the formation of plumboferrite ($PbFe_4O_7$ or $PbO{\cdot}2Fe_2O_3$) is the reason for inhibition. However, this is not possible to confirm from the XRD results, since the signal from the lead species seen in Figure 4.23 and 4.24 is not strong enough to determine what kind of species it is. From the XPS results, the dominant peak in the iron surface is a Pb^{2+} peak. It is likely to assume that this is PbO, but it could be due to another Pb^{2+} component such as plumboferrite. Lead oxide can also be present in the iron oxide matrix as another plumbeous component, or just as random segregated PbO. In both cases, it is possible that lead oxide will improve the protective properties of the oxide. Mayne [4] observed a growth of the thickness of the surface oxide of steel by 7.2-16.9%, submerged in a

solution contain lead. This number was calculated from potential measurement and therefore the observation can result from a denser or less porous oxide rather than a thicker oxide. This could simply be due to the presence of lead oxide, which may affect the potential without affecting the oxide thickness.

A third possible mechanism is that the deposited metallic lead blocks the redox reaction. This effect was observed by Jüttner [29] in an acidic environment, where metallic lead hinders hydrogen evolution on cathodic sites. However, a part of the assumed protection mechanism for this system is that the lead prevents anodic dissolution. The prevention of anodic dissolution is though to be due to a formation of a dense lead layer, which slows down the migration of ferrous ions. The main argument against this theory is the low quantity of lead found in the outer oxide layer. A quantity of around 2at% is probably not enough to bring about inhibition of corrosion.

Summarised, since metallic lead is observed, it is a necessity that the lead acts as the cathode at some point in time. Therefore, it is possible that protection due to depolarisation of reduction reaction is contributing to inhibit corrosion. Anodic protection is a likely protection mechanism. However, several of the mechanisms can be a part of the true protection mechanism. Lead oxide can strengthen the protective surface oxide and metallic lead deposits can act as a barrier for anodic dissolution of iron at anodic sites and at slow down cathodic reduction. The fact that both metallic lead and PbO is present in the surface oxide supports that other mentioned mechanisms inhibit corrosion, in addition to anodic protection.

5.5 Further Work

One of the stated ambitions from the preliminary project was to remove the paint mechanically. However, the proposed methods in that report did not work, with the exception for the epoxy paint (Sample 4). During the project, liquid nitrogen was suggested for the mechanical removal of the paint. The result of this is shown in Figure 5.1 and should be sufficient for examination in XPS. The preparation of the samples is described in Appendix A. A test of an unexposed sample should also be included in this test. This could explain the formation of the unknown lead species found both in the paint and the surface of steel exposed for paint (Figure 4.1 and 4.4). It can be assumed that this species is formed from ionic lead present in a water phase, and the unexposed sample will thus not have a single XPS peak located at approximately 138.8eV. If this peak is observed, it will be a strong indication that lead soaps play an important role in the access of ionic lead.

Another important aspect is to repeat the same test as for Sample 2, 3 and 4, just with the use of liquid nitrogen instead of removal with a thinner as described in section 3.2.1.

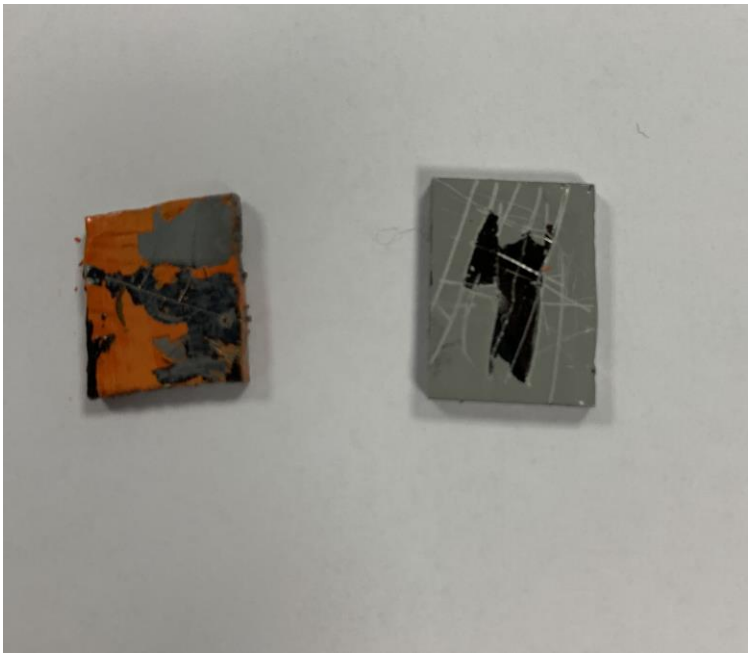

Figure 5.1: Removed paint with the use of liquid nitrogen. Test samples.

An interesting concern is to find the reason for why the potential of the passivated steel surface has dropped between the first test and the second (Figure 4.14 and 4.18). Experiments with the attempt to find out if it is the thickness or the exposure for a humid environment that is responsible for the drop in the potential, could be helpful. The observed raise in potential of the passivated steel area during the second test of Sample 11 (Figure 4.20), could also be of interest.

6. Conclusion

Metallic lead and lead monoxide are observed in the protective oxide of moderately moisture exposed steel samples painted with LBP. A concentration of lead of 2.22 atomic percent is found in the outer part of the oxide, and the concentration is decreasing through the oxide. It is likely that inhibition of corrosion is due to the presence of these lead species in the iron oxide.

Inhibition of corrosion with the use of LBP can be related to an increase in the corrosion potential from the equilibrium potential of -0.44V vs. SHE to the observed corrosion potential around -0.225 to -0.270V vs. SHE. This potential can be related to the reduction of ionic lead to metallic lead at a concentration of around 10^{-4}M. Metallic lead seems to originate from the cathodic deposition of lead ions in the electrolyte, but could be from a reduction of lead(II)oxide.

Since metallic lead seems to be cathodically deposited, the anodic current will increase due to depolarisation of the cathodic reduction. This could lead to anodic protection of steel.

Another possible explanation for corrosion protection is inhibition of anodic and cathodic sites by metallic lead. Secondly, improved properties of the protective oxide due to the presence of lead oxide, which can e.g. lead to a high resistance film.
It should be stressed that a combination of two or all of the proposed mechanisms can bring about inhibition of corrosion with the use of LBP.

References

1. Golden Gate Bridge Highway and Transportation District. *Frequently Asked Question about the Golden Gate Bridge*. [Access date: 13.05.2019]; Tilgjengelig fra: http://www.goldengatebridge.org/research/facts.php - painting.
2. Alter, C. *Glolden Gate Bridge Closing for Fisrt Time in Decades*. 2015 [Access date: 12.05.2015]; Tilgjengelig fra: http://time.com/3661935/golden-gate-bridge-closure-traffic/.
3. Statens vegvesen, *Private Photo*.
4. Appleby AJ and Mayne JEO, *Corrosion inhibition by salts of long chain fatty acids.* Journal of the Oil and Chemists´ Association, 1967. **50**(10): p. 897-.
5. Kjøraas, E., *The Protective Mechanism of Lead Based Paint*. 2018, Norwegian University of Science and Technology: Trondheim. p. 29.
6. Forsgren A and Knudsen OØ, *Corrosion control through organic coating*. 2017: CRC Press.
7. Revie RW. and Uhlig HH., *Corrosion and corrosion control: an introduction to corrosion science and engineering*. 4 ed. 2008, New Jersey, USA: John Wiley and Sons.
8. Bardal, E., *Korrosjon og korrosjonsvern*. 2. utg. ed. 1994, Trondheim: Tapir.
9. International Organization for Standarization, *ISO 12944-5. Paint and varnishes - Corrosion protection of steel structures by protective paint systems. Part 5: Protective paint systems. .* ISO 12944-5. 2007, Geneva.
10. Reidar Klinge, *Personal Communication*. Statens vegvesen
11. Svoboda M and Mleziva J, *Properties of coatings determined by anticorrosive pigments.* Progress in Organic Coatings, 1984. **12**: p. 261-271.
12. Mckinley JP. Dalaska MK. Batson R., *Red lead: understanding red lead in lead– acid batteries.* Journal of power sources, 2002. **107**(2): p. 180-186.
13. Blackman AG. Gahan LR. Aylward G. and Findlay T., *Aylward and Findlay´s SI chemical data*. 7 ed. 2014, Australia: John Wilson and Sons.
14. Brokbartold M. Temminghoff EJM. Weng L. and Marschener B., *Unique characteristics of Pb in soil contaminated by red lead anti-corrosion paint.* Soil and Sediment Contamination: An International Journal 2013. **22**(8): p. 839-855.

15. Delahay P. Pourbaix M. and Rysselberghe PV., *Potential - pH Diagram of Lead and its Applications to the Study of Lead Corrosion and to the Lead Storage Battery.* Journal of The Electrochemical Society, 1951. **98**(2): p. 57-64.
16. Mickalonis J and Leidheiser Jr H, *The Mechanism of Corrosion Inhibition by Lead Pigment in Organic Coatings*, in *Corrosion control through a better understanding of the metallic substrate/organic coating interface*. 1989, Lehigh University Bethlehem. p. 23.
17. Lindqvist S-Å and Vannerberg N-G, *Corrosion-inhibiting properties of red lead-I. Pigment suspensions in aqueous solutions.* Material and Corrosion 1974. **25**(10): p. 740-748.
18. Thomas NL, *THE PROTECTIVE ACTION OF RED LEAD PIGMENT ALKYDS ON RUSTED MILD STEEL.* Proceeding of the Symposium on Advances in Corrosion Protection by Organic Coatings, 1989. **89**(13): p. 451.
19. Thomas NL, *The barriere properties of paint coatings.* Progress in Organic Coatings 1991. **19**: p. 101.
20. Mayne JEO. Turgoose S. and Wilson JM., *Detection of Lead, by Auger Spectroscopy, on Iron inhibited in Lead Azelate Solution.* British Corrosion Journal, 1973. **8**(5): p. 236-237.
21. Appleby AJ and Mayne JEO, *The relative protection afforded by red lead dispersed in linseed oil, tung oil, oiticica oil and a long alkyd varnish.* Journal of the Oil and Chemists´ Association, 1976. **59**(2): p. 69-71.
22. Mayne JEO., *The protective action of lead compounds.* Journal of the Society of Chemical Industry, 1946. **65**(7): p. 196-204.
23. Mayne JEO and Van Rooyen D, *The mechanism of the corrosion inhibitive action of paints, with special reference to basic pigments.* Journal of Applied Chemistry, 1954. **4**(7): p. 384-394.
24. National Center for Biotechnology Information. *1,3-Dioxa-2lambda2-plumbacyclododecane-4,12-dione*. [Access date: 10.06.2019]; Tilgjengelig fra: https://pubchem.ncbi.nlm.nih.gov/compound/129678889.
25. Yao Y. Murphy A. *Investigating the Formation and Structure og Lead Soaps in Traditional Oil Paintings*. [Access date: 10.06.2019]; Tilgjengelig fra: https://www.metmuseum.org/about-the-met/conservation-and-scientific-research/projects/lead-soaps.

26. Mayne JEO and Ramshaw EH, *Autoxidation of the lead soaps of the linseed oil fatty acids.* Journal of Applied Chemistry 1963. **13**: p. 553
27. Pryor MJ., *The Protective Action of Pigments on Steel.* Journal of The Electrochemical Society, 1954. **101**(3): p. 141-148.
28. Lindqvist, S.-Å., *Corrosion inhibiting properties of red lead. Chatalytic activity of metallic lead in the oxide layer on steel due to a polarity change in the bimetal couple lead-steel.* Journal of the Oil and Chemists´ Association 1984. **67**(11): p. 288-292.
29. Jüttner K, *The inhibiting effect of underpotential metal deposits on iron corrosion.* Material and Corrosion, 1980. **31**(5): p. 358-363.
30. Vetere VF and Romagnoli R, *Study of the heterogeneous reaction between iron and lead oxides.* Journal of Chemical Technology and Biotechnology, Chemical Technology, 1985. **35**(3): p. 97-107.
31. Kim KS. O´leary TJ., *X-Ray Photoelectron Spectra of Lead Oxides.* Analytical Chemistry, 1973. **45**(13): p. 2214-2218.
32. Okamoto Y. Carter WJ. Hercules DM., *A Study of the Interaction of Pb-Sn Solder with O 2, H 2 O, and NO 2 by X-ray Photoelectron (ESCA) and Auger (AES) Spectroscopy.* Applied Spectroscopy 1979. **33**(3): p. 287-293.
33. Naumkin AV. Kraut-Vass. A. Gaarenstroom SW. Powell CJ. *NIST X-ray Photoelectron Spectoscopy Database*. 2012 [Access date: 10.06.2019]; Tilgjengelig fra: https://srdata.nist.gov/xps/.
34. Nazarov AP and Thierry D, *Studies in the Electrical Double Layer at Metal/Polymer Interfaces by Scanning Capacitive Probe.* Protection of metals, 2003. **39**(1): p. 55-62.
35. ICDD, *International Centre for Diffraction Data.* 2019, Newtown Square, PA, USA.
36. Didziulis SV and Fleischauer PD, *Chemistry of the Extreme-Pressure Lubricant Additive Lead Naphtenate on Steel Surfaces* Langmuir, 1991. **7**(12): p. 2981-2990.
37. Sababi M. Terryn H. and Mol JMC., *The influence of a Zr-based conversion treatment on interfacial bonding strength and stability of epoxy coated carbon steel.* Progress in Organic Coatings, 2017. **105**: p. 29-36.
38. Chen C. Mansfeld F., *Potential distribution in the Evans drop experiment.* Corrosion Science, 1997. **39**(2): p. 409-413.

39. Khun NW. Frankel GS., *Khun, N. W., & Frankel, G. S. (2013). Effects of surface roughness, texture and polymer degradation on cathodic delamination of epoxy coated steel samples.* Corrosion Science, 2013. **67**: p. 152-160.
40. Zavieh AH. Espallargas N, *The effect of friction modifiers on tribocorrosion and tribocorrosion-fatigue of austenitic stainless steel.* Tribology International, 2017. **111**: p. 138-147.

Appendix A: Preparation of XPS Samples With Liquid Nitrogen

The steel is prepared according to subsection 3.1. LBP (*MINIO DI PIOMBO RED LEAD PRIMER*®) or Epoxy (JOTAMASTIC 87 STD038®) is applied to the samples with a brush. Samples 5,6 and 7 are left to dry for two days before they are baked (furnace: Fermaks) at 40˚C for three days. Sample 5 and 6 are exposed in a moisture chamber (Vötsch VC 0057) at 40°C and 82% relative humidity for 8 days. Sample 7 is not exposed in the moisture chamber.

The paint on Sample 5, 6 and 7 are removed with the use of liquid nitrogen. The samples are cooled down in a beaker containing liquid nitrogen for some minutes (2 to 3 minutes). The samples are subsequently scratched with a sharp metal tip. Due to this scratch, the brittle paint will break off in flakes and leave behind a big enough clean steel surface for examination.

Sample 11 is cut out from an SKP sample. The sample is prepared as described in section 3.4 and exposed as described in Table 3.2. The sample was cut out to a XPS specimen with a small manual iron saw. The sample is cut as gently as possible out of the original SKP sample, to avoid heating of the sample due to friction.

Table B.1: Schematic overview of XPS samples.

Sample	Examined in:	Paint	Environmental Exposure	Removal of paint
5	XPS	LBP	82RH, 40°C, for 8 days	By liquid nitrogen
6	XPS	Epoxy	82RH, 40°C, for 8 days	By liquid nitrogen
7	XPS	LBP	None	By liquid nitrogen
11	SKP XPS	LBP	- 95RH, 25°C, for 121 days - 3,5wt% NaCl reservoir + 95RH, 25°C. For 161 days.	- By liquid nitrogen

Appendix B: Scanning Kelvin Probe Results From Second Test

Figure B.1 shows the whole scan length of Sample 11 during the second test round, before the CD scan. As seen in Figure B.1, the potential before the CD scan shows a higher potential close to the damage, compared to the middle part of the scan length. This could be due to a thicker coating since a "cut" in the paint will make an edge, which will be thicker than the rest of the coating. The rapid increase in potential from about 6000µm to 8000µm is remarkable. The whole stripe of paint is measured to approximately 9mm. The increase in potential could be due to the damage on the other side of the paint, or another area, which has a different thickness. Figure B.2 shows the whole scan length of Sample 11 during the second CD test.

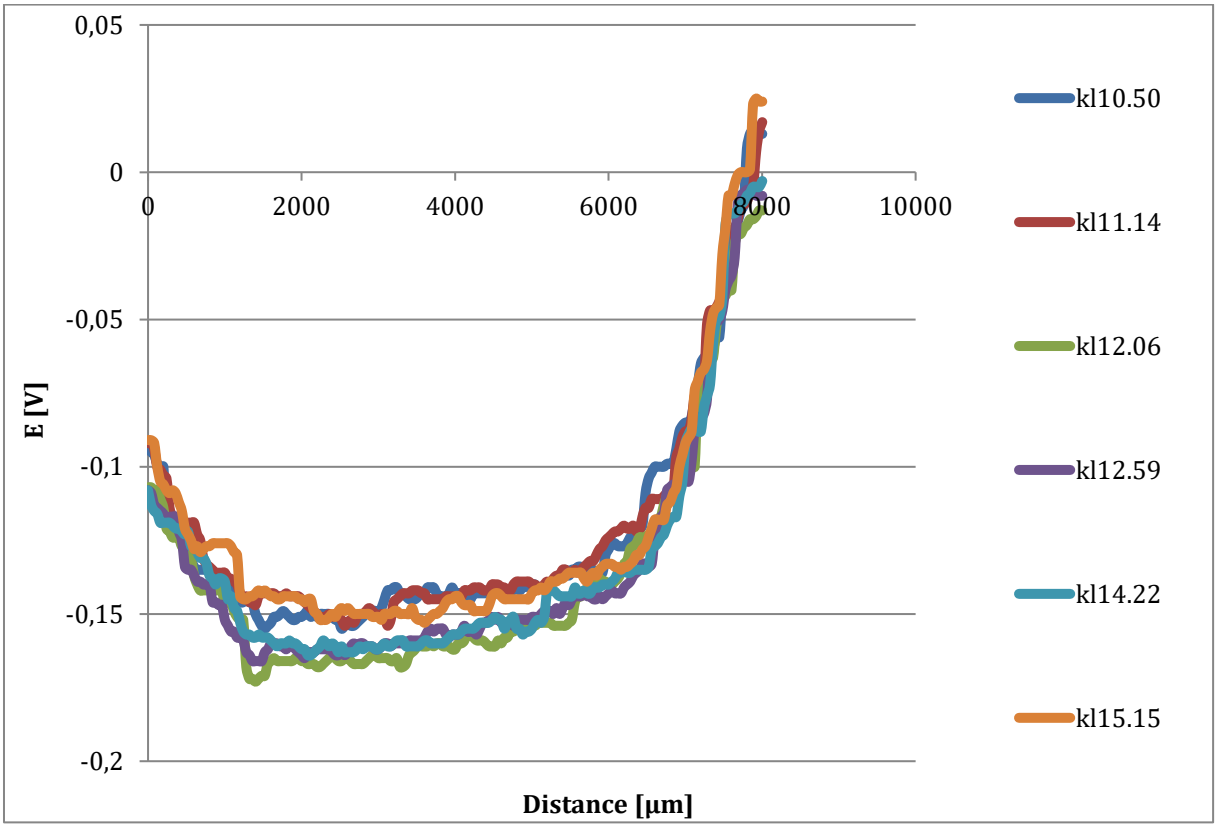

Figure B.1: Measured potential before the CD test of Sample 11. The whole scan length.

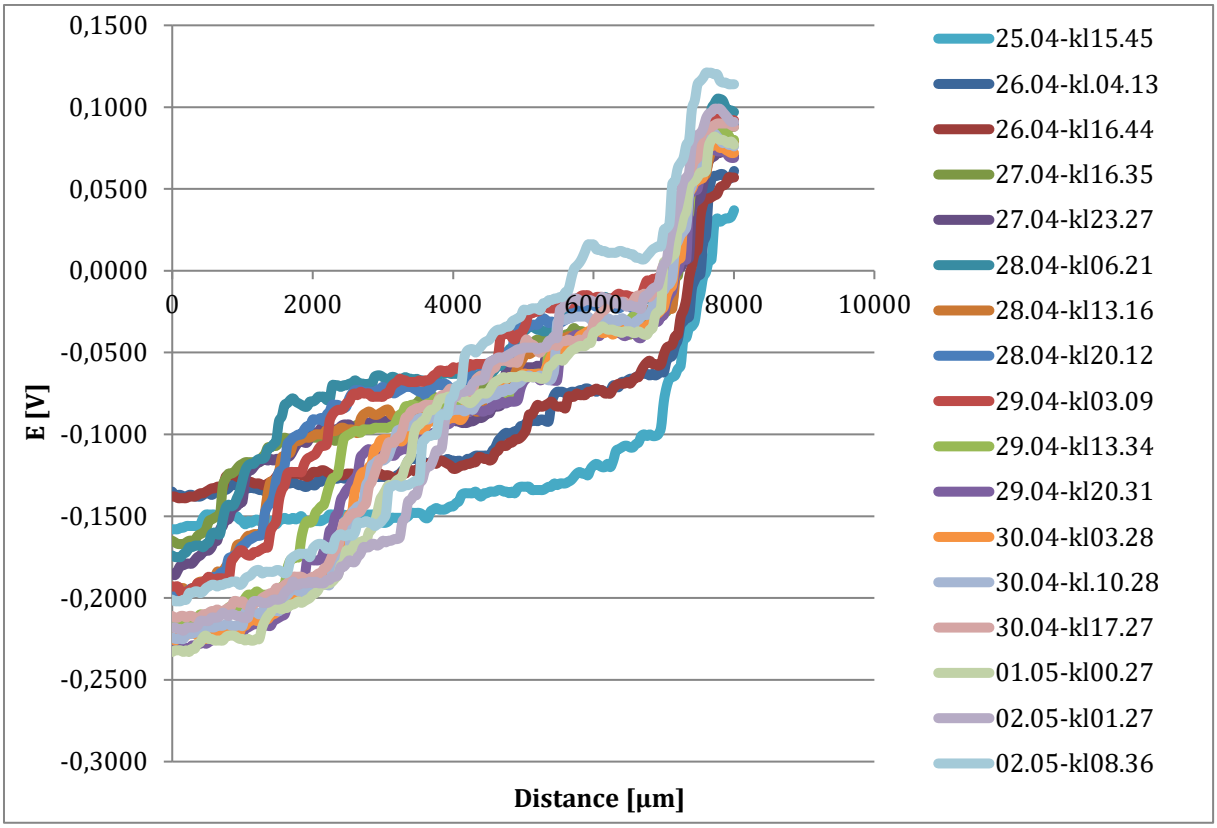

Figure B.2: CD test of Sample 11. Second test round. Whole scan length.

Appendix C: Iron peaks from X-ray Photoelectron Spectroscopy

As seen from Figure C.1 to C.9 the steel which has been painted with LBP seems to have more metallic Fe in the outermost oxide. Table C.1 shows the location of the different iron peaks from before sputtering until 15s with sputtering. Table C.2 shows the distribution from 115s sputtering to 615 seconds sputtering. Notice the shift for the metallic iron peak from 706.8eV to 707.2eV in Table C.1 and C.2. The reported values is according to previous literature [5, 33, 40]. This shift is due to the lack of oxide species at depth from 115 seconds of sputtering and deeper. When both metallic and oxides species are present they will repel each other to some degree, and consequently lead to a shift when the concentration of one of them goes toward zero. From 115 seconds with sputtering (Figure C.10 to C.15), no difference between the peaks is observed for all of the samples.

Table C.1: Identification of iron species from 0 to 15 seconds of sputtering time.

	Fe Metallic	FeO	Fe_3O_4	Fe^{3+}
Binding energy (eV)	706.8 +/- 0.2	709-710	711-711.5	713-713,5
FWHM	0.9	2.4	2.4	3.6

Table C.2: Identification of iron species from 115 to 615 seconds of sputtering time.

	Fe Metallic	FeO	Fe_3O_4	Fe^{3+}
Binding energy (eV)	707.2 +/- 0.2	709.4-710.4	711.4-711.9	713.4-713,9
FWHM	0.9	2.4	2.4	3.6

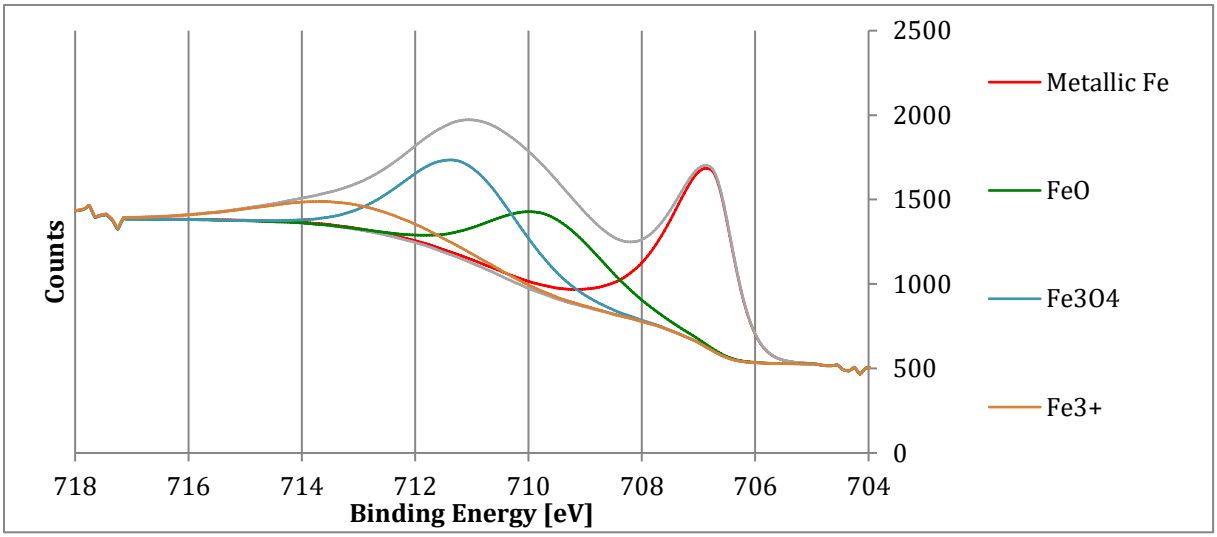

Figure C.1: LBP, 0 seconds sputtering time. Sample 2.

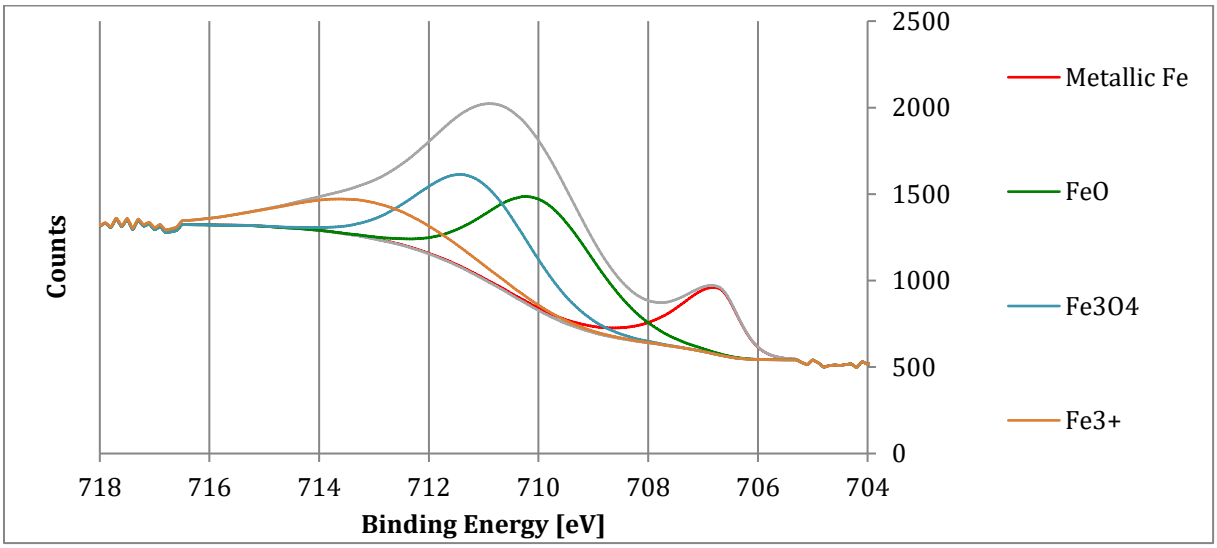

Figure C.2: Steel, 0 seconds sputtering time. Sample 1.

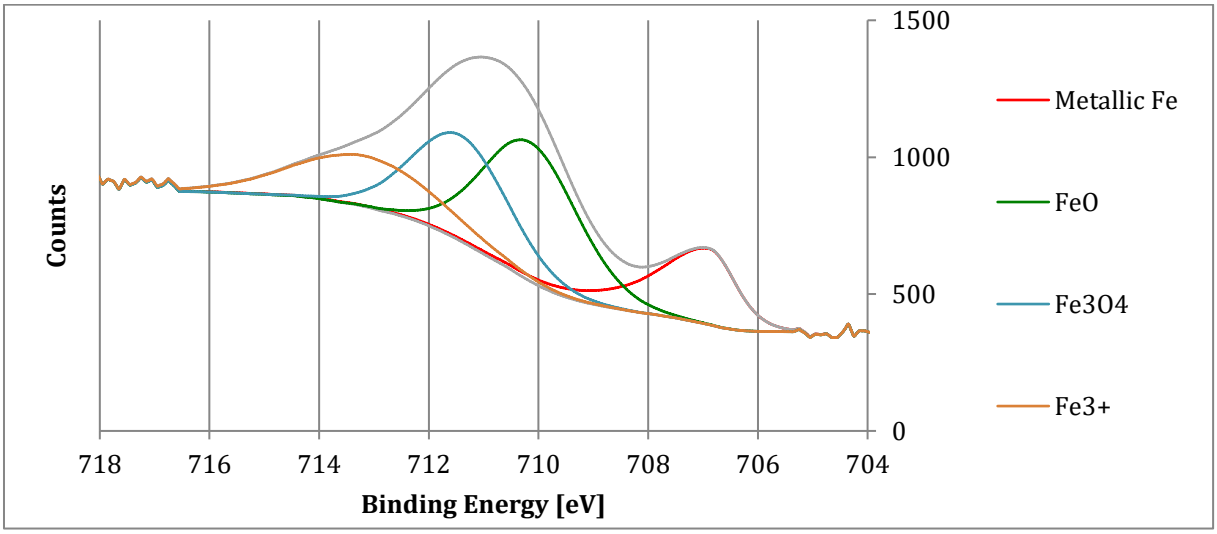

Figure C.3: Epoxy, 0 seconds sputtering time. Sample 4.

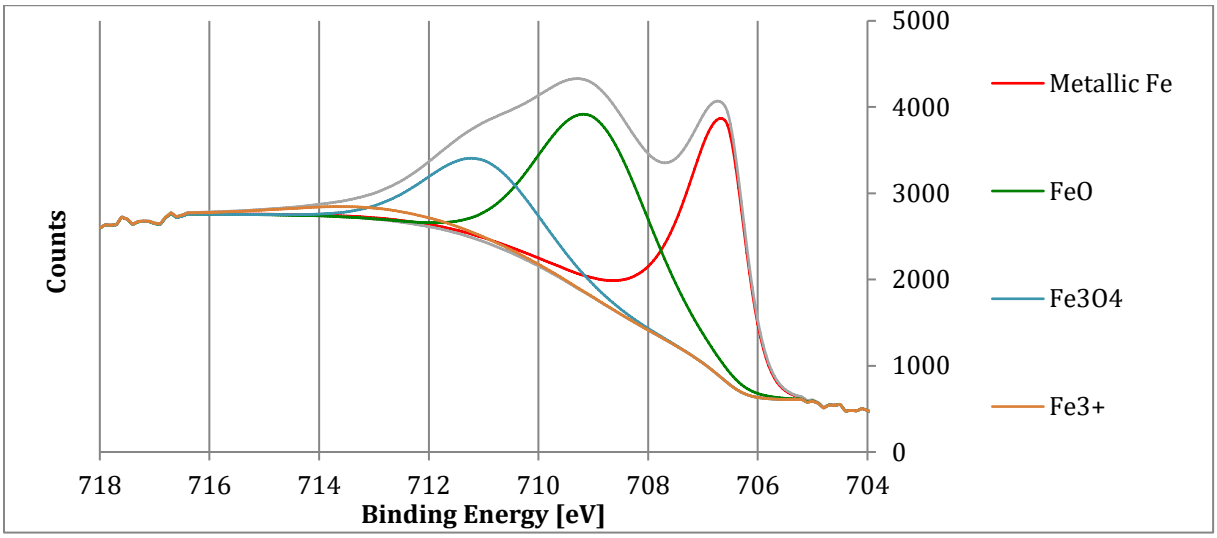

Figure C.4: LBP, 5 seconds sputtering time. Sample 2.

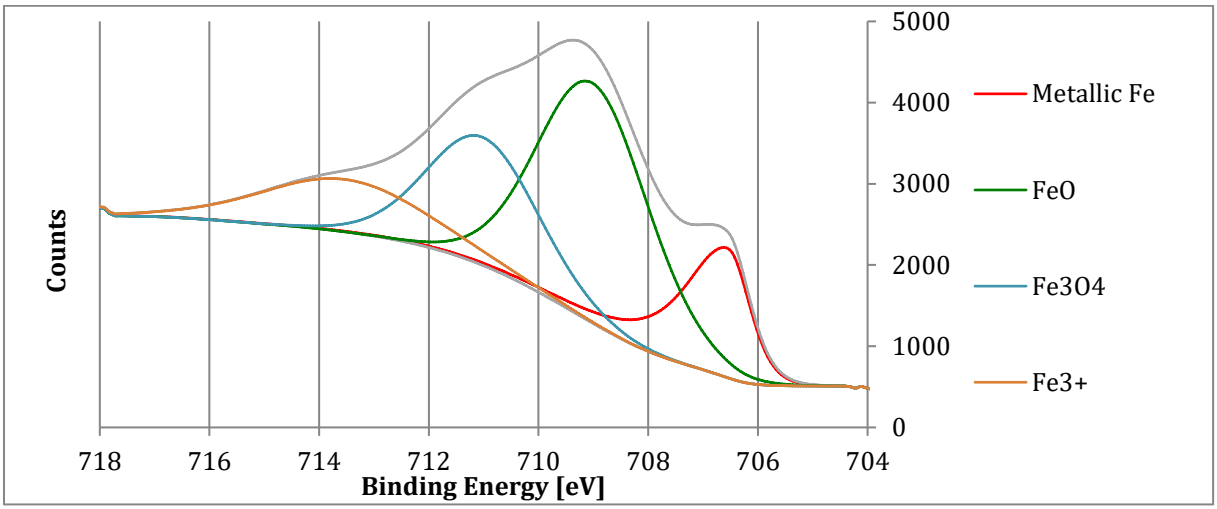

Figure C.5: Steel, 5 seconds sputtering time. Sample 1.

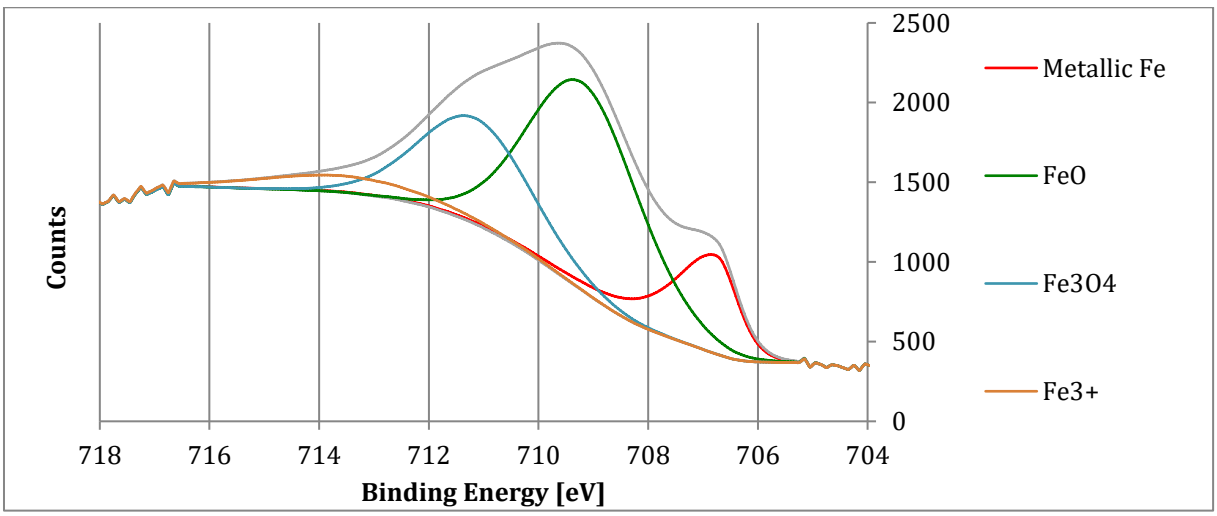

Figure C.6: Epoxy, 5 seconds sputtering time. Sample 4.

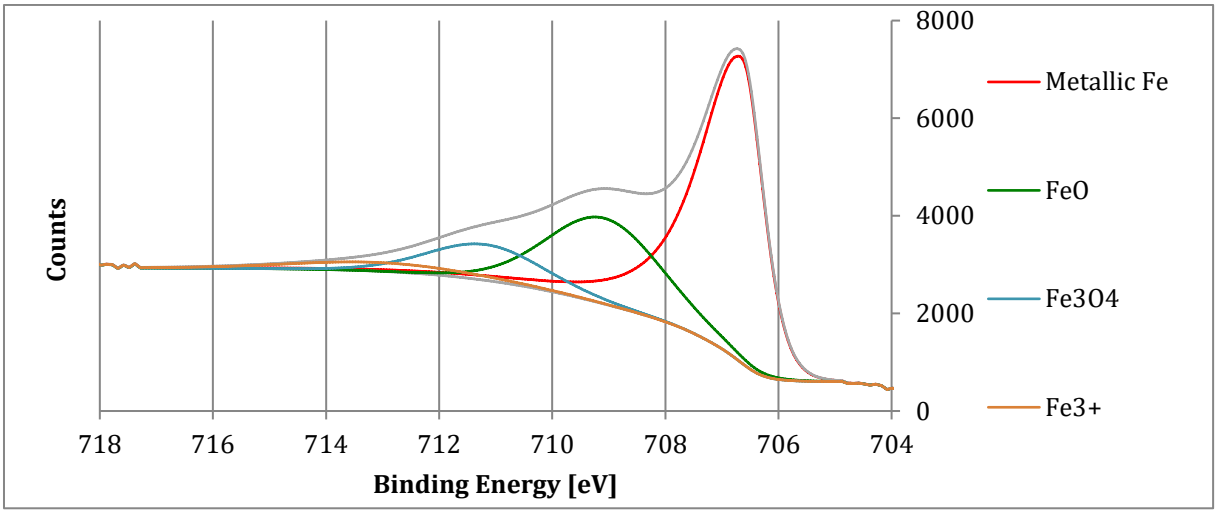

Figure C.7: LBP 15 seconds sputtering time. Sample 2.

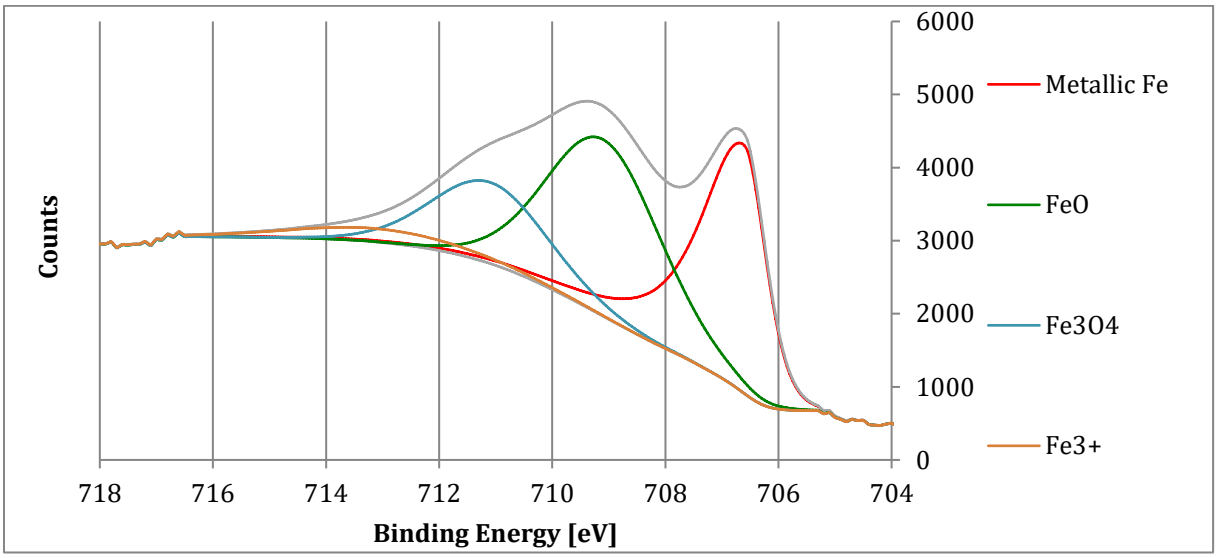

Figure C.8: Steel, 15 seconds sputtering time. Sample 1.

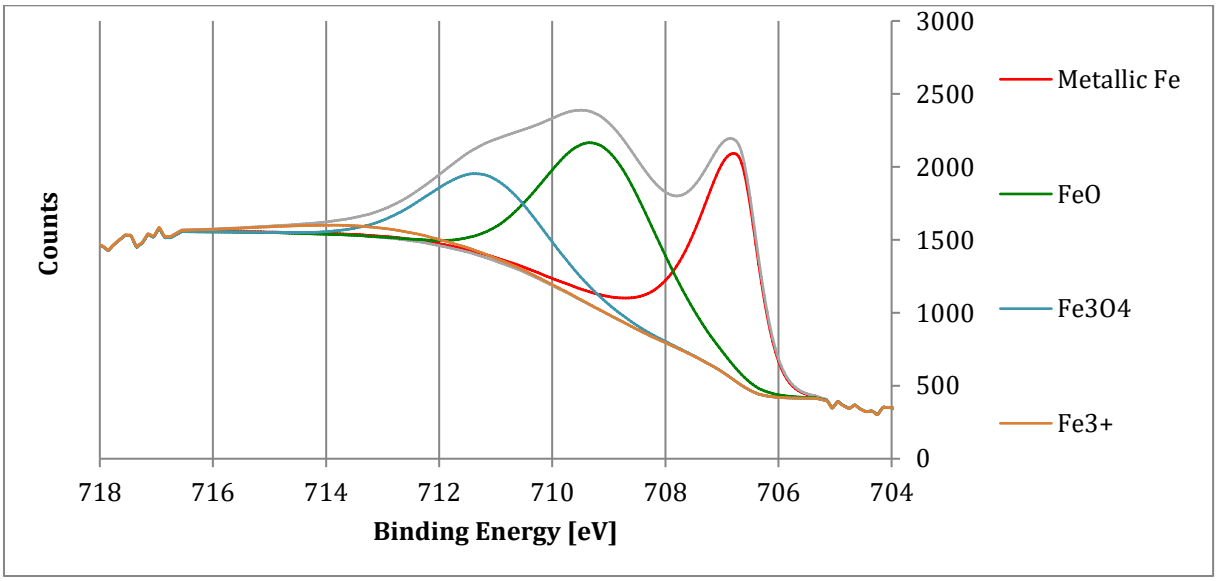

Figure C.9: Epoxy, 15 seconds sputtering time. Sample 4.

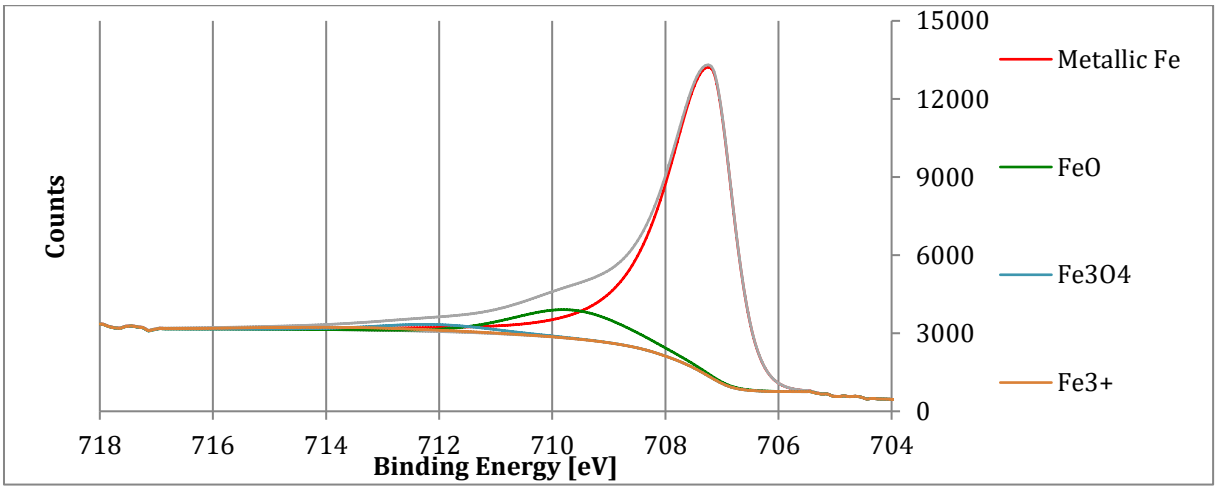

Figure C.10: LBP, 115 seconds sputtering time. Sample 2.

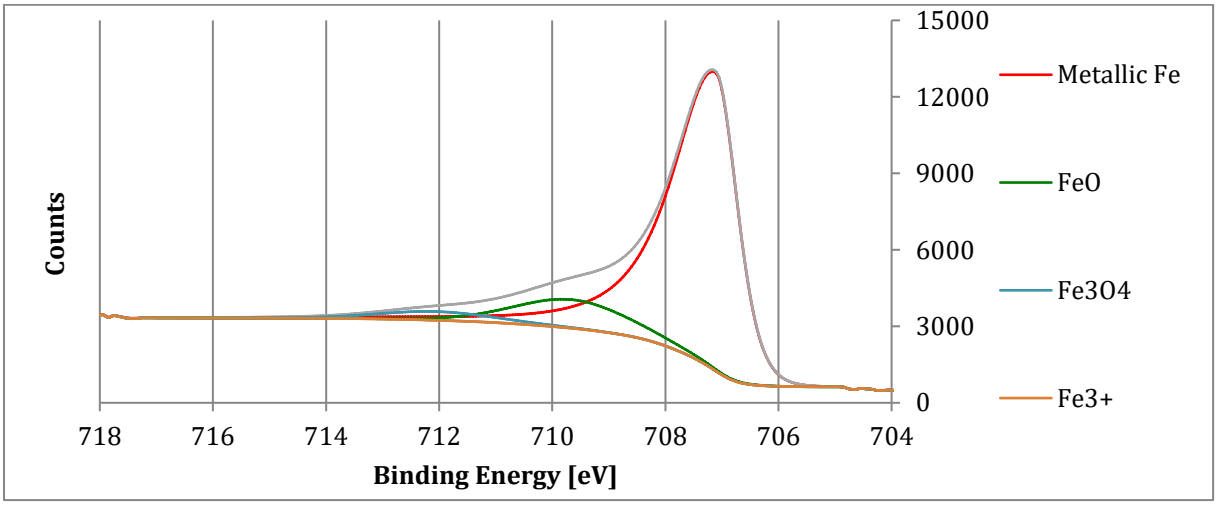

Figure C.11: Steel, 115 seconds sputtering time. Sample 1.

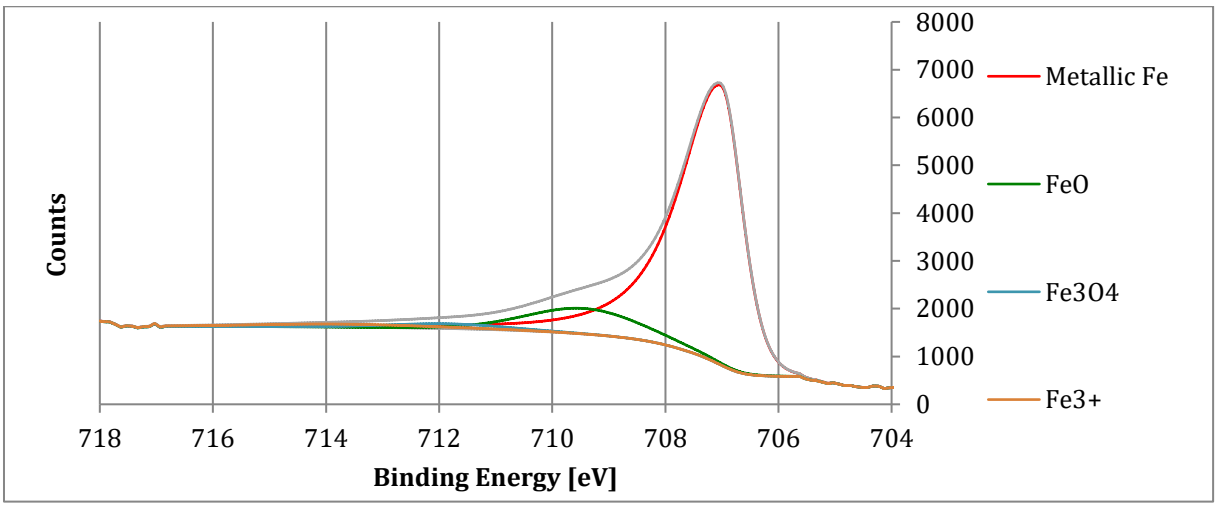

Figure C.12: Epoxy, 115 seconds sputtering time. Sample 4.

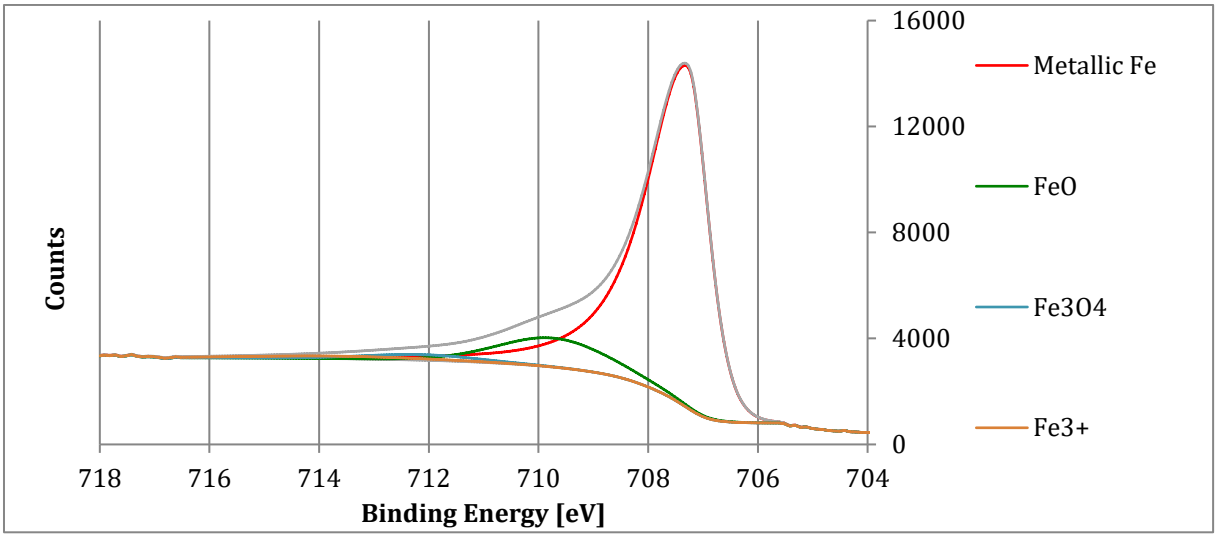

Figure C.13: LBP, 615 seconds sputtering time. Sample 2.

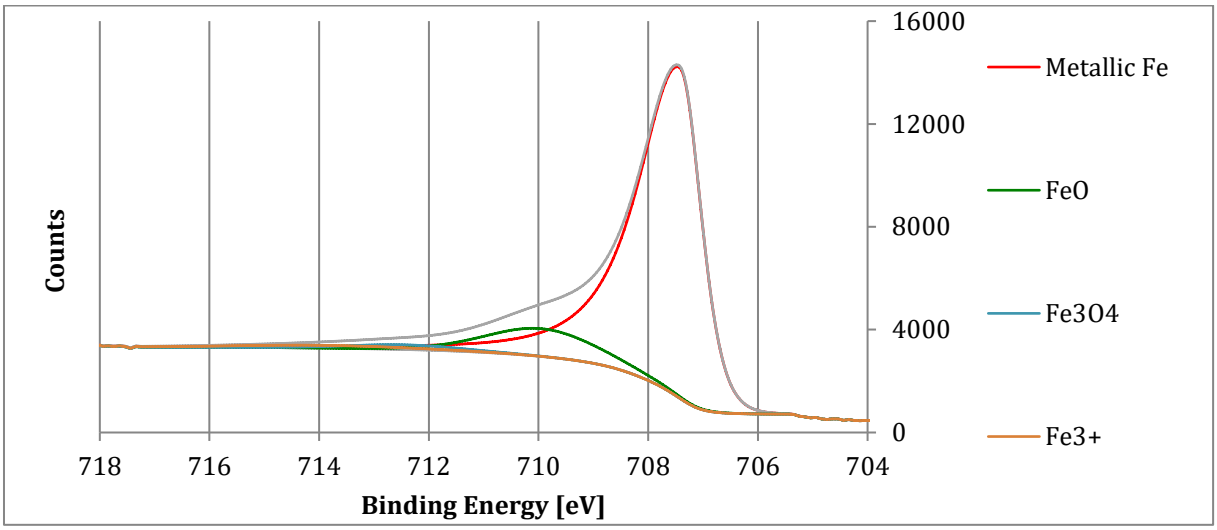

Figure C.14: Steel, 615 seconds sputtering time. Sample 1.

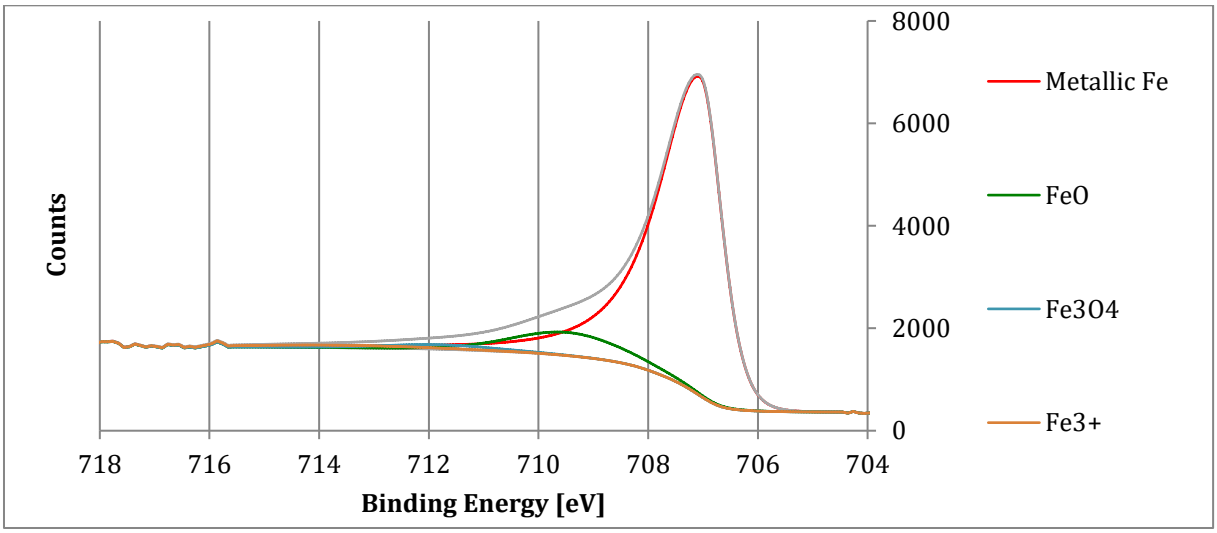

Figure C.15: Epoxy, 615 seconds sputtering time. Sample 4.

Appendix D: Copy of Risk Assessment

ID	30742	**Status**	**Dato**
Risikoområde	Risikovurdering: Helse, miljø og sikkerhet (HMS)	Opprettet	01.10.2018
Opprettet av	Erlend Kjøraas	Vurdering startet	01.10.2018
Ansvarlig	Ole Øystein Knudsen	Tiltak besluttet	
		Avsluttet	24.10.2018

Risikovurdering:

Blymønje

Gyldig i perioden:
10/1/2018 - 10/1/2021

Sted:
Perleporten/Nanolaben

Mål / hensikt
Karakterisere oksidbelegg under blymønje. Blymønje er giftig.

Bakgrunn
Karakterisering av oksidbelegget på stål ved hjelp av XPS. Prøvene vil være finpolerte stålprøver, som deretter males (blymønje) og utsettes for lett korrosivt miljø. Malingsbelegget fjernes og oksidbelegget blir undersøkt i XPS.

Beskrivelse og avgrensninger
- Polering av stålprøver
- Påføring av blymønje
- Eksponering av prøvene i lett korrosivt miljø (fra noen timer til et døgn eller to).
- Fjerning av blymønje
- Undersøkelse i XPS.

Forutsetninger, antakelser og forenklinger
Arbeidet med påføring og fjerning av blymønjen utføres i avtrekksskap. I henhold til sikkerhetsdatablad skal vernebriller, ansiktsmaske og hansker brukes. Avfall fra eksponering i korrosivt miljø skal samles opp.

Vedlegg
Sikkerhetsdatablad Pb3O4.pdf

Referanser
[Ingen registreringer]

Knudsen Ole Øystein

Digitally signed by Knudsen Ole Øystein
DN: cn=Knudsen Ole Øystein
Date: 2019.06.07 01:21:31 +02'00'

Oppsummering, resultat og endelig vurdering

I oppsummeringen presenteres en oversikt over farer og uønskede hendelser, samt resultat for det enkelte konsekvensområdet.

Farekilde: **Påføring og fjerning av blymønje**

Uønsket hendelse: **Innånding**

Konsekvensområde: Helse — Risiko før tiltak:  Risiko etter tiltak: 

Uønsket hendelse: **Søl**

Konsekvensområde: Helse — Risiko før tiltak:  Risiko etter tiltak: 

Uønsket hendelse: **Spill**

Konsekvensområde: Ytre miljø — Risiko før tiltak:  Risiko etter tiltak: 

Farekilde: **Eksponering i korrosivt miljø.**

Uønsket hendelse: **Lekasje av partikler til ytre miljø.**

Konsekvensområde: Helse — Risiko før tiltak:  Risiko etter tiltak: 
Ytre miljø — Risiko før tiltak:  Risiko etter tiltak: 

Farekilde: **Polering av stålprøver og XPS**

Uønsket hendelse: **Skader på materiell**

Skal ikke analyseres.

Endelig vurdering

Det jobbes med små mengder bly. Og vurderte tiltak sees på som tilstrekkelig for å hindre eksponering.

Involverte enheter og personer

En risikovurdering kan gjelde for en, eller flere enheter i organisasjonen. Denne oversikten presenterer involverte enheter og personell for gjeldende risikovurdering.

Enhet /-er risikovurderingen omfatter

- Institutt for materialteknologi

Deltakere

Erlend Kjøraas

Lesere

[Ingen registreringer]

Andre involverte/interessenter

Ole Øystein Knudsen - Veileder
Amin Hossein Zavieh - Veileder

Følgende akseptkriterier er besluttet for risikoområdet Risikovurdering: Helse, miljø og sikkerhet (HMS):

Helse	Materielle verdier	Omdømme	Ytre miljø
			

Oversikt over eksisterende, relevante tiltak som er hensyntatt i risikovurderingen

I tabellen under presenteres eksisterende tiltak som er hensyntatt ved vurdering av sannsynlighet og konsekvens for aktuelle uønskede hendelser.

Farekilde	Uønsket hendelse	Tiltak hensyntatt ved vurdering
Påføring og fjerning av blymønje	Innånding	Vernebriller
	Innånding	Ansiksmaske
	Innånding	Hansker
	Innånding	Avtrekkskap
	Søl	Vernebriller
	Søl	Ansiksmaske
	Søl	Hansker
	Søl	Oppsamling av avfall
	Spill	Avtrekkskap
Eksponering i korrosivt miljø.	Lekasje av partikler til ytre miljø.	Vernebriller
	Lekasje av partikler til ytre miljø.	Ansiksmaske
	Lekasje av partikler til ytre miljø.	Hansker
	Lekasje av partikler til ytre miljø.	Avtrekkskap

Eksisterende og relevante tiltak med beskrivelse:

Vernebriller
I henhold til sikkerhetsdatablad

Ansiksmaske
I henhold til sikkerhetsdatablad

Hansker
I henhold til sikkerhetsdatablad

Avtrekkskap
Arbeid med påføring og fjerning av blymønje gjennomføres i avtrekkskap.

Oppsamling av avfall
Alt som har vært i kontakt blymønje skal samles opp og blir deretter tatt hånd om av SINTEF.

Risikoanalyse med vurdering av sannsynlighet og konsekvens

I denne delen av rapporten presenteres detaljer dokumentasjon av de farer, uønskede hendelser og årsaker som er vurdert. Innledningsvis oppsummeres farer med tilhørende uønskede hendelser som er tatt med i vurderingen.

Følgende farer og uønskede hendelser er vurdert i denne risikovurderingen:

- **Påføring og fjerning av blymønje**
  - Innånding
  - Søl
  - Spill
- **Eksponering i korrosivt miljø.**
  - Lekasje av partikler til ytre miljø.

Detaljert oversikt over farekilder og uønskede hendelser:

Farekilde: Påføring og fjerning av blymønje

Blymønje (Pb3O4) er meget giftig. Kan føre til blyforgiftning.

Uønsket hendelse: Innånding

Kan føre til blyforgifting (akkutt eller kroniske skader som følge av inntak).

Sannsynlighet for hendelsen (felles for alle konsekvensområder): **Svært lite sannsynlig (1)**

Kommentar:

Mengdene maling (blymønje) er små. Redusernede tiltak vil gi tilstrekkelig beskyttelse.

Konsekvensområde: Helse

Risiko:

Vurdert konsekvens: **Svært stor (4)**

Kommentar: Er meget giftig. Ved absorbasjon av bly i kroppen kan det føre til blyforgiftning, noe som kan føre til nerveskader og kreft. Akutt blyforgiftning kan føre til død.

Uønsket hendelse: Søl

Vil være skadelig i kontakt med hud.

Sannsynlighet for hendelsen (felles for alle konsekvensområder): **Svært lite sannsynlig (1)**

Kommentar:

Små mengder blymøjne skal brukes. Nødvendig beskyttelse brukes for å hindre evt. søl på hud.

Konsekvensområde: Helse

Risiko:

Vurdert konsekvens: **Middels (2)**

Kommentar: Kan føre til blyforgiftning ved svelging eller kontakt med hud.

Uønsket hendelse: Spill

Kan være skadelig om lekasje til avløpssystemer.

Sannsynlighet for hendelsen (felles for alle konsekvensområder): **Svært lite sannsynlig (1)**

Kommentar:

Arbeid gjennomføres i lukket miljø.

Konsekvensområde: Ytre miljø

Risiko:

Vurdert konsekvens: **Middels (2)**

Kommentar: Kan gi skader på dyrelivet om lekkasjer til naturen, spesielt i vann. Iht sikkerhetsdatablad.

Farekilde: Eksponering i korrosivt miljø.

Blymønje (Pb3O4) er meget giftig. Kan føre til blyforgiftning.

Uønsket hendelse: Lekasje av partikler til ytre miljø.

Blymønje (Pb3O4) er meget giftig. Kan føre til blyforgiftning.

Sannsynlighet for hendelsen (felles for alle konsekvensområder): **Svært lite sannsynlig (1)**

Kommentar:

Bruk av beskyttelseutstyr vil redusere faren for at partikkler kan ble eksponert for kroppen. Arbeid skjer i lukket system.

Konsekvensområde: Helse

Risiko:

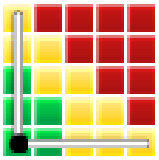

Vurdert konsekvens: **Liten (1)**

Kommentar: Eksponering mot herdet blymønje er ikke antatt å være skadelig. Det er arbeid i forbindelse med påføring og fjerning som er forbunnet med eksponering.

Konsekvensområde: Ytre miljø

Risiko:

Vurdert konsekvens: **Middels (2)**

Kommentar: Partikkler kan lekke ut i avløp, selv om dette ikke er forventet.

Oversikt over besluttede risikoreduserende tiltak:

Under presenteres en oversikt over risikoreduserende tiltak som skal bidra til å reduseres sannsynlighet og/eller konsekvens for uønskede hendelser.

Detaljert oversikt over besluttede risikoreduserende tiltak med beskrivelse:

Detaljert oversikt over vurdert risiko for hver farekilde/uønsket hendelse før og etter besluttede tiltak